Proteomics data reveals Wnt signaling involvement in the hippocampal-dependent behavioral impairment in THRSP-overexpressing attention-deficit/hyperactivity disorder mouse model

Raly James Custodio
Leibniz Research Centre for Working Environment and Human Factors
Hee Jin Kim
Sahmyook University
Jiyeon Kim
Seoul National University
Darlene Mae Ortiz
Sahmyook University https://orcid.org/0000-0001-5377-3785
Mikyung Kim
Sahmyook University https://orcid.org/0000-0003-0524-1658
Danilo Buctot
Sahmyook University
Leandro Val Sayson
Sahmyook University https://orcid.org/0000-0003-3475-5527
Hyun Jun Lee
Sahmyook University
Bung-Nyun Kim
Seoul National University
Eugene Yi
Seoul National University
Jae Hoon Cheong (rjampc@outlook.com)
Jeonbuk National University https://orcid.org/0000-0001-5654-5868

Article

Keywords: ADHD predominantly inattentive, Hippocampus, Neuronal Markers, Thyroid hormone-responsive protein (THRSP), Wnt signaling

Posted Date: July 28th, 2022

DOI: https://doi.org/10.21203/rs.3.rs-1885484/v1

Version of Record: A version of this preprint was published at Communications Biology on January 16th, 2023. See the published version at https://doi.org/10.1038/s42003-022-04387-5.

Abstract

Despite the predominance and high heritability of attention-deficit/hyperactivity disorder (ADHD), its etiology remains unclear. Preclinical and clinical evidence partially implicates impaired limbic system function, particularly in the hippocampus (HPC). Children diagnosed with ADHD often struggle with deficits in executive function, temporal processing, and visuospatial memory, the defining hallmarks of the predominantly inattentive presentation (ADHD-PI), which is subserved by the hippocampus. However, the specific genes/proteins involved and how they shape hippocampal structure to influence ADHD behavior remain poorly understood. As an exploratory tool, hippocampal tissues from a mouse model overexpressing (OE) thyroid hormone-responsive protein (THRSP) with defining characteristics of ADHD-PI were utilized for proteomic analyses. Integrated proteomics and network analysis revealed altered protein network involved in Wnt signaling. Compared with THRSP knockout (KO) mice, THRSP OE mice showed impaired attention and memory, accompanied by dysregulated Wnt signaling affecting hippocampal cell proliferation (BrdU) and neurogenic marker expression (i.e., NEU-N, GFAP), markers of neural stem cell (NSC) activity. In addition, combined exposure to an enriched environment and treadmill exercise could improve behavioral deficits in THRSP OE mice and Wnt signaling and NSC activity.

Introduction

Attention-deficit/hyperactivity disorder (ADHD) is a heterogeneous neurodevelopmental condition characterized by a ubiquitous array of inattention, impulsivity, and hyperactivity behaviors typically diagnosed in children [1] and often persist into adulthood [2]. According to global estimates, ADHD affects 8–12% of children [3] and 2–6% of adults [4]. Moreover, twin and adoption studies have indicated that ADHD is a highly heritable disorder, with heritability estimated between 77–90% [5, 6], suggesting the substantial role of genetics in the etiology of ADHD. However, no single gene can predict this disorder. Conversely, numerous studies have indicated that approximately 33% of ADHD heritability may be caused by polygenic factors comprising several common variants, each with a small effect size [7]. Furthermore, considerable evidence supports the interaction between genetic (polygenic) and environmental factors during early development [8, 9, 10].

Studies have implicated widespread changes in the brain macro- and microstructure, including the frontal, basal ganglia, anterior cingulate, temporal, and parietal regions [11, 12], with high associations in the left parahippocampal gyrus [13] and hippocampus (HPC) [14, 15, 16, 17, 18, 19]. Children diagnosed with ADHD frequently struggle with deficits in executive function, temporal processing, and visuospatial memory, the defining hallmarks of predominantly inattentive presentation (ADHD-PI) [20, 21, 22, 23], considered to be subserved by the hippocampal region.

The HPC comprises two layers of neurons, pyramidal neurons in the cornu ammonis (CA) and granule neurons in the dentate gyrus (DG) fields [24]. This brain region is involved in consolidating emotional memory and episodic memory formation. Interestingly, the hippocampal DG can generate new neurons

throughout life in humans [25, 26, 27] and rodents [28, 29], termed adult neurogenesis [30, 31, 32] and believed to play a crucial role in cognitive plasticity [33]. Interestingly, alterations during neurogenesis and plasticity of the developing brain and later in life are often discussed as vulnerability factors for developing psychiatric disorders such as ADHD [34, 35]. Recently, personalized fingerprinting of the brain functional connectome has revealed sensitive time points in brain maturation and plasticity that differed from those with symptoms of ADHD [36, 37]. Evidence indicates that candidate risk genes in ADHD are enriched in pathways such as neurite outgrowth, axon guidance, cell trafficking, brain development, and neurogenesis [38, 39, 40], all of which are regulated by Wnt signaling [41, 42, 43, 44].

Extracellular Wnt signaling stimulates numerous intracellular signaling cascades that regulate crucial aspects of neural stem cell (NSC) fate determination, cell migration, cell polarity, neural patterning, and organogenesis [45] during embryonic and adult brain development [46] via the transcriptional coactivator catenin beta 1 (β-catenin; Ctnnb1), which forms the Wnt/β-catenin signaling pathway. Given this extensive range of roles, dysregulation of Wnt signaling could have pathological effects on neurodevelopment [47]. Previous findings have afforded new hypotheses: Apart from the well-recognized multifactorial ADHD etiological factors, recent evidence proposes that the interface between genetic and environmental factors and particularly Wnt signaling pathways might significantly contribute to ADHD pathophysiology [10, 34, 48, 49, 50, 51].

In an extension of our previous studies and for preclinical exploration of the genetic underpinnings of ADHD, the present study performed proteomic analysis of the HPC of a thyroid hormone-responsive protein (THRSP)-overexpressing (OE) mouse model of predominantly inattentive ADHD (ADHD-PI) presentation. This ‘bottom-up’ experimental approach is intended to screen and identify enriched pathways, particularly those involved in Wnt signaling, which could further elucidate the ADHD-PI endophenotype observed in THRSP OE mice. We also evaluated the effects of environmental enrichment on behavior and gene expression.

Materials And Methods

Animals

Herein, we used two THRSP transgenic mouse lines, OE and knockout (KO) mice [52] and their wild-type (WT) counterparts (Figure 1a), confirmed using DNA electrophoresis (genotyping). These lines were continuously bred and maintained at the Uimyung Research Institute for Neuroscience (Laboratory of Pharmacology, Sahmyook University) [52, 53] animal facility until the appropriate experimental age was reached. In addition, non-transgenic littermates were used as WT counterparts. Briefly, mice were housed in a temperature- and humidity-controlled environment (temperature, 22 ± 2°C; relative humidity, 55 ± 5%) under a 12/12 h light/dark (07:00–19:00 h light) cycle. All standard animal care and procedures were performed following the Principles of Laboratory Animal Care (NIH Publication No. 85-23, revised 1985), the Animal Ethics Review Board of Sahmyook University, South Korea (SYUIACUC2020-010), and in

compliance with the 3Rs framework [54] and ARRIVE guidelines [55] recommended by *Nature Communications*.

EXPERIMENT 1: Evaluation of potential genetic targets affecting ADHD-PI behavior

Y-maze

Prior to proteomic and other molecular analyses of the hippocampal region, 7-week-old mice (between postnatal [PND] 49 or 50) (n=12) were examined in the Y-maze test to confirm the impaired behavior (i.e., inattention, impaired memory) in adult THRSP OE and the absence thereof in THRSP KO mice, compared with WT mice, which were previously observed [52, 53]. The use of 7-week-old or PND 49 or 50 mice was based on a previous study that identified the chronometry of species, indicating full body growth completion by PND 50 [56]. Accordingly, we employed an arbitrary date of PND 49 or 50 as a reasonable age for an adult mouse.

Briefly, each mouse was placed in one arm of the Y-maze (45 × 10 × 20 cm), allowed to explore freely for 10 min, and recorded using Ethovison XT (RRID: SCR_000441; Noldus, Netherlands). 'Arm entry' was defined as entry of all four paws (mice) into an arm and the 'alternation behavior' (actual alternations) as a consecutive entry into three arms. The percentage of spontaneous alternation was calculated as the ratio of actual alternations to the maximum number of alternations (total number of arm entries minus two) multiplied by 100 (% alternation = [(number of alternations)/(total arm entries − 2)] × 100).

Separate groups of mice (n=12) maintained in a standard environment (SE) (6 per cage) or enriched environment (EE) (6 per cage) were subjected to Y-maze tests at a frequency of four tests conducted on days 7, 14, 21, and 28 in the reared environment (Figure 7a).

Brain extraction

In the first set of experiments, brain samples from 18 mice (Figure 1a) were randomly assigned for use in proteomics analysis, quantitative reverse transcription-polymerase chain reaction (qRT-PCR), western blotting, or immunofluorescence (Figure 4-6). For the first six samples, HPC was divided into left and right portions, in which the left hippocampal side of the brain was snap-frozen and enclosed in a dry ice-filled box, subsequently transported to the SNU laboratory for proteomic analysis. The remaining right half was prepared for protein extraction and underwent western blotting. We used the second set of six hippocampal brain samples for qRT-PCR and the last six brain samples for immunofluorescence targeting the hippocampal DG.

Proteomic analysis

Proteins were extracted from mouse HPC brain tissues using radioimmunoprecipitation assay (RIPA) buffer and quantified using the bicinchoninic acid protein assay. Briefly, 200 μg of each sample were resolved by sodium dodecyl sulfate (SDS)-polyacrylamide gel electrophoresis under reducing conditions and stained with Instant Blue Coomassie protein stain. Each lane was divided into 10 individually

processed segments for in-gel protein digestion. Stained gel fragments were cut into small pieces, washed with 100 mM ammonium bicarbonate (NH4HCO3), and dehydrated with 50% (v/v) acetonitrile (ACN) in 25 mM ammonium bicarbonate. The reduction was performed by incubating samples with 20 mM dithiothreitol (DTT) for 1 h at 60°C, followed by alkylation with 55 mM iodoacetamide for 45 min in the dark. After washing and dehydration with acetonitrile, gel pieces were covered with 12.5 ng/μL trypsin in 50 mM NH4HCO3, and digestion was performed overnight at 37°C. Peptide extraction was carried out by incubation at 37°C with 10% formic acid (FA) and further incubation with 50% ACN in 0.1% FA and 80% ACN in 0.1% FA. Eluted peptides were dried in a SpeedVac and stored at −20°C until further use.

Liquid Chromatography with tandem mass spectrometry (LC/MS/MS) and data analysis

Peptides were resuspended in solvent A (0.1% FA), loaded into an analytical column, and separated with a linear grade 5–35% solvent B (0.1% FA in 98% ACN) for 95 min at a flow rate of 300 nL/min. The MS spectra were recorded on a Q-Exactive plus hybrid quadrupole-orbitrap MS coupled with an Ultimate 3000 HPLC system. The standard mass spectrometric condition of the spray voltage was set to 2.0 kV, and the temperature of the heated capillary was set to 250°C. Full scans were acquired in the range of 400–1400 m/z with 70,000 resolutions, and the normalized collision energy was 27% and 17,500 resolutions for high-energy collision dissociation fragmentation. The data-dependent acquisition was performed with a single survey MS scan, followed by 10 MS/MS scans with a dynamic exclusion time of 30 s. The collected MS/MS raw data were converted into mzXML files using engine-based PEAKS Studio. Protein identification was performed using the UniProt-Musculus database, setting the precursor mass tolerance to 10 ppm and fragment mass tolerance to 0.8 Da. Oxidized methionine was considered a variable amino acid modification, and carbamidomethylation of cysteine was deemed a fixed modification. Trypsin was selected as the enzyme, allowing up to two missed cleavages. Peptide and protein identifications were further filtered to < 1% FDR, as measured using a concatenated target-decoy database search strategy. Relative protein quantitation samples were analyzed using the Power Law Global Error Model (PLGEM) (http://www.bioconductor.org) package within the R program (version 3.4.2). PLGEM can control datasets to distinguish statistically significant DEPs and calculate expression level changes by p-value and signal-to-noise ratio. Ingenuity pathway analysis was performed using all significantly altered proteins.

Gene ontology (GO) analysis

Analyses of GO biological processes and enriched pathways were performed using the GENEONTOLOGY/PANTHER classification system (v.17) [57, 58, 59]. We used upregulated and downregulated DEPs from THRSP KO and OE mice relative to WT mice to analyze GO biological processes. In contrast, the total DEPs (upregulated and downregulated) were used for GO enrichment analysis.

Search Tool for the Retrieval of Interacting Genes/Proteins (STRING) analysis

To investigate the biological relevance of identified DEPs, protein-protein interaction networks were generated using STRING (v.11.5) [60]. The graphical representation of protein networks was restricted to

high-confidence interactions with a score interaction threshold of 0.9, excluding non-interacting proteins.

RNA extraction and qRT-PCR

Total RNA was isolated using TRIzol (Invitrogen, Carlsbad, CA, USA). A Hybrid-RTM Kit (Geneall Biotechnology, Seoul, Korea) was used for RNA purification. The total RNA concentration was determined with a Colibri Microvolume Spectrometer (Titertek-Berthold, Pforzheim, Germany).

qRT-PCR was used to measure mRNA expression levels of Thrsp and those involved in Wnt signaling (upstream/downstream), based on our previous report [61]. One microgram (μg) of total RNA was reverse-transcribed into cDNA using AccuPower CycleScript RT Premix (Bioneer, Seoul, Korea). The cDNA amplification was performed using custom-made sequence-specific primers (Cosmogenetech, Seoul, Korea) (Thyroid hormone-responsive protein (Thrsp), F: 5'-ATGCAAGTGCTAACGAAACGC-3', R: 5'-CCTGCCATTCCTCCCTTGG-3'; Wnt family member 3 (Wnt3), F: 5'-CTCGCTGGCTACCCAATTTG-3', R: 5'-CTTCACACCTTCTGCTACGCT-3'; Wnt family member 4 (Wnt4), F: 5'-AGACGTGCGAGAAACTCAAAG-3', R: 5'-GGAACTGGTATTGGCACTCCT-3'; Wnt family member 6 (Wnt6), F: 5'-GCAAGACTGGGGGTTCGAG-3', R: 5'-CCTGACAACCACACTGTAGGAG-3'; Wnt family member 7a (Wnt7a), F: 5'-TCAGTTTCAGTTCCGAAATGGC-3', R: 5'- CCCGACTCCCCACTTTGAG-3'; Wnt family member 8b (Wnt8b), F: 5'-CCCGTGTGCGTTCTTCTAGTC-3', R: 5'-AGTAGACCAGGTAAGCCTTTGG-3'; Wnt family member 11 (Wnt11), F: 5'-GCTGGCACTGTCCAAGACTC-3', R: 5'-CTCCCGTGTACCTCTCTCCA-3'; Cerberus 1 (Cer1), F: 5'-CTCTGGGGAAGGCAGACCTAT-3', R: 5'-CCACAAACAGATCCGGCTT-3'; Dickkopf Wnt signaling pathway inhibitor 1 (Dkk1), F: 5'-CTCATCAATTCCAACGCGATCA-3', R: 5'-GCCCTCATAGAGAACTCCCG-3'; Dickkopf Wnt signaling pathway inhibitor 4 (Dkk4), F: 5'-GTACTGGTGACCTTGCTTGGA-3', R: 5'-CCGTTCATCGTGAAACGCTAAG-3'; Secreted frizzled related protein 2 (sFrp2), F: 5'-CGTGGGCTCTTCCTCTTCG-3', R: 5'-ATGTTCTGGTACTCGATGCCG-3'; Secreted frizzled related protein 5 (sFrp5), F: 5'-CACTGCCACAAGTTCCCCC-3', R: 5'-TCTGTTCCATGAGGCCATCAG-3'; Shisa family member 4 (Shisa4), F: 5'-GGACTGCTTGTGGTATCTGGA-3', R: 5'-CGGTGATGAGTAAGGTCAGGT-3'; Shisa family member 9 (Shisa9), F: 5'-CTCCTGTCGGGGCTACTTC-3', R: 5'-CCGCTTCTTAAACGTGCAGC-3'; Insulin like growth factor binding protein 1 (Igfbp1), F: 5'-ATCAGCCCATCCTGTGGAAC-3', R: 5'-TGCAGCTAATCTCTCTAGCACTT-3'; Insulin like growth factor binding protein 1 (Igfbp5), F: 5'-CCCTGCGACGAGAAAGCTC-3', R: 5'-GCTCTTTTCGTTGAGGCAAACC-3'; Wnt inhibitory factor 1 (Wif1), F: 5'-TCTGGAGCATCCTACCTTGC-3', R: 5'-ATGAGCACTCTAGCCTGATGG-3'; Sclerostin (Sost), F: 5'-AGCCTTCAGGAATGATGCCAC-3', R: 5'-CTTTGGCGTCATAGGGATGGT-3'; Sclerostin domain containing 1 (Sostdc1), F: 5'-CCTGCCATTCATCTCTCTCTCA-3', R: 5'-CCGGGACAGGTTTAACCACA-3'; Adenomatosis polyposis coli downregulated 1 (Apcdd1), F: 5'-CTTCACGGCGTCCAAGTCAT-3', R: 5'-GCAAGTTCGGTTCACCAGTC-3'; Frizzled class receptor 1 (Fzd1), F: 5'-CAGCAGTACAACGGCGAAC-3', R: 5'-GTCCTCCTGATTCGTGTGGC-3'; Frizzled class receptor 3 (Fzd3), F: 5'-ATGGCTGTGAGCTGGATTGTC-3', R: 5'-GGCACATCCTCAAGGTTATAGGT-3'; Low density lipoprotein receptor-related protein 1 (Lrp1), F: 5'-ACTATGGATGCCCCTAAAACTTG-3', R: 5'-GCAATCTCTTTCACCGTCACA-3'; Low density lipoprotein receptor-related protein 5 (Lrp5), F: 5'-AAGGGTGCTGTGTACTGGAC-3', R: 5'-AGAAGAGAACCTTACGGGACG-3'; Low density lipoprotein receptor-related protein 6 (Lrp6), F: 5'-

TTGTTGCTTTATGCAAACAGACG-3', R: 5'-GTTCGTTTAATGGCTTCTTCGC-3'; Low density lipoprotein receptor-related protein 10 (Lrp10), F: 5'-GGATCACTTTCCCACGTTCTG-3', R: 5'-GAGTGCAGGATTAAATGCTCTGA-3'; Receptor tyrosine kinase like orphan receptor 1 (Ror1), F: 5'-TGAGCCGATGAATAACATCACAA-3', R: 5'-CAGGTGCATCATTCTTGAACCA-3'; Receptor tyrosine kinase like orphan receptor 2 (Ror2), F: 5'-ATCGACACCTTGGGACAACC-3', R: 5'-AGTGCAGGATTGCCGTCTG-3'; Receptor like tyrosine kinase (Ryk), F: 5'-GGTCTTGATGCAGAGCTTTACT-3', R: 5'-CCCATAGCCACAAAGTTGTCTAC-3'; Disheveled segment polarity protein 1 (Dvl1), F: 5'-ATGAGGAGGACAATACGAGCC-3', R: 5'-GCATTTGTGCTTCCGAACTAGC-3'; Disheveled segment polarity protein 2 (Dvl2), F: 5'-GGTGTAGGCGAGACGAAGG-3', R: 5'-GCTGCAAAACGCTCTTGAAATC-3'; Disheveled segment polarity protein 3 (Dvl3), F: 5'-GTCACCTTGGCGGACTTTAAG-3', R: 5'-AAGCAGGGTAGCTTGGCATTG-3'; Axin 2 (Axin2), F: 5'-TGACTCTCCTTCCAGATCCCA-3', R: 5'-TGCCCACACTAGGCTGACA-3'; Adenomatous polyposis coli regulator of Wnt signaling pathway (Apc), F: 5'-CTTGTGGCCCAGTTAAAATCTGA-3', R: 5'-CGCTTTTGAGGGTTGATTCCT-3'; Apc regulator of Wnt signaling pathway 2 (Apc2), F: 5'-CACACAGTTTGACCATCGTGA-3', R: 5'-GTGGACGAGGTTGCGTAGC-3'; Casein kinase 1 alpha 1 (Csnk1α1), F: 5'-TCCAAGGCCGAATTTATCGTC-3', R: 5'-ACTTCCTCGCCATTGGTGATG-3'; Casein kinase 1 epsilon (Csnk1ε), F: 5'-ATGGAGTTGCGTGTGGGAAAT-3', R: 5'-ACATTCGAGCTTGATGGCTACT-3'; Glycogen synthase kinase 3 beta (Gsk3β), F: 5'-TGGCAGCAAGGTAACCACAG-3', R: 5'-CGGTTCTTAAATCGCTTGTCCTG-3'; Catenin beta 1 (Ctnnβ1), F: 5'-ATGGAGCCGGACAGAAAAGC-3', R: 5'-CTTGCCACTCAGGGAAGGA-3';) and was detected with SYBR Green (Solgent, Korea).

qRT-PCR analysis was performed in duplicate, and values were normalized to mRNA levels of the housekeeping gene Actin beta (Actb), F:5’- GGCTGTATTCCCCTCCATCG-3’, R:5’-CCAGTTGGTAACAATGCCATGT-3’]. The relative expression levels were calculated using the $2^{-\Delta\Delta Ct}$ method.

Western blotting

Western blotting was performed to evaluate the expression levels of specific Wnt signaling targets and neuronal markers in the mouse hippocampal region. Western blotting protocols were performed in accordance with those utilized in our previous studies [53, 62]. Briefly, 30 µg of protein lysates were loaded and electrophoresed on 10% sodium dodecyl sulfate and polyacrylamide gels and subsequently transferred onto nitrocellulose membranes. Membranes were blocked with 5% bovine serum albumin in Tris-buffered saline with Tween-20 (TBST) for 1 h and incubated overnight with the following primary antibodies: rabbit polyclonal anti-phosphorylated-GSK3B (1/1000; Cell Signaling Technology Cat# 9336, RRID:AB_331405), rabbit monoclonal anti-GSK3B (1/1000; Cell Signaling Technology Cat# 9336, RRID:AB_331405), rabbit polyclonal anti-CSNK1E (1/1000; Cell Signaling Technology Cat# 12448, RRID:AB_2797919), rabbit polyclonal anti-GFAP (1/1000; LSBio, catalog number: LS-B15993), mouse monoclonal anti-NEU-N (1/1000; LSBio [LifeSpan] Cat# LS-C312122, RRID:AB_2827517). The standard control was performed using mouse monoclonal anti-ACTB (1/5000; Sigma-Aldrich Cat# A5441, RRID:AB_476744). Subsequently, the blots were washed in TBST and incubated with the appropriate

HRP-conjugated anti-rabbit (Bio-Rad Cat# 170-6515, RRID:AB_11125142) and anti-mouse (Bio-Rad Cat# 170-6516, RRID:AB_11125547) secondary antibodies for 1 h. After three final washes with TBST, blots were visualized using enhanced chemiluminescence (Clarity Western ECL; Bio-Rad Laboratories) in a ChemiDoc Imaging System (Bio-Rad ChemiDoc MP Imaging System, RRID:SCR_019037).

5-BrdU injection

To label cell proliferation or mitotic cells in naïve mice, all groups were injected with 50 mg/kg 5-Bromo-2-deoxyuridine (5-BrdU) (Cat# HY-15910 MedChemExpress, Monmouth Junction, NJ, USA) once daily for 6 days. On the last day (day 7), all groups were injected with 100 mg/kg 5-BrdU after behavioral experiments or 3 h prior to brain extraction. 5-BrdU was dissolved in 0.7% dimethyl sulfoxide (DMSO) and 1% Tween-80 in 0.9% saline solution and administered intraperitoneally (i.p.).

Immunofluorescence

Briefly, 5-BrdU-injected mice (n=6/group) were sacrificed immediately after the last day of the respective experiments. Standard protocols for brain fixation were followed [63]. Briefly, mice were anesthetized using tiletamine/zolazepam (50 $mg \cdot mL^{-1}$); Zoletil; Vibrac Laboratories, Carros, France) and xylazine (100 $mg \cdot mL^{-1}$). Using the intracardiac route, mice were perfused with a perfusion solution (0.05 M phosphate-buffered saline [PBS] and perfusate [4% paraformaldehyde; PFA] in 0.1 M phosphate buffer [PB]). Subsequently, mouse brains were carefully isolated, placed in a PFA solution-filled container, and stored at 4°C. The following day, brain samples were washed with PBS to remove the excess PFA, placed in a 30% sucrose solution, and stored at 4°C until use.

Brain samples were sectioned using a cryostat (Leica CM1850; Wetzlar, Germany) adjusted to 40-µm thickness, following stereotaxic coordinates of the mouse brain [64]. The brain slices were placed in a 0.2 M PB:distilled water:ethylene glycol:glycerin (1:3:3:3) storage solution and stored at 4°C (short-term storage) or -20°C (long-term storage).

The hippocampal region, specifically the DG, was selected, given its neurogenic role in the adult brain [65]. Brain slices were carefully washed thrice in a 24-well plate filled with 1× PBS. Subsequently, samples were incubated in a protein-blocking solution (5% goat serum and 0.3% Triton™ X-100 in 1× PBS) for 1 h at room temperature. Thereafter, brain slices were incubated (free-floating) with primary antibodies (dilution, 1/250) dissolved in a protein-blocking solution for 3 days. The primary antibodies used were mouse monoclonal anti-BrdU (Thermo Fisher Scientific, Cat# MA3-071, RRID:AB_10986341), mouse monoclonal anti-NEU-N (LSBio, Cat# LS-C312122, RRID:AB_2827517), and rabbit polyclonal anti-GFAP (LSBio; catalog number: LS-B15993). After thrice washing with 1× PBS, the samples were incubated with either goat-anti-rabbit Alexa Fluor™-555 or goat-anti-mouse Alexa Fluor™-488 dyes (1/250) overnight at room temperature. The samples were thrice washed in 1× PBS and then incubated for 10 min with Hoechst 33342 (Thermo Scientific, MA, USA; catalog number:62249) in 1× PBS (1/1000). After three final washes with 1× PBS, the brain slices were mounted on 25 × 75 × 1 mm clean positively charged

microscope slides (Walter Products Inc., MI, USA; catalog number: C17090W) and cured with Fisher Chemical™ Permount™ Mounting Medium (Fisher Scientific, NH, USA; catalog number: SP15-100). The prepared slides were then covered with 24 × 50 mm microscope cover glasses (Marienfield Laboratory Glassware, Germany; catalog number:0101222) and observed under a confocal laser-scanning microscope (Leica TCS SP8). The number of cells expressing BrdU in the DG was counted, and corrected cell fluorescence levels for NEU-N and GFAP in the DG were analyzed using ImageJ software (RRID: SCR_003070), as described previously [63, 66, 67].

EXPERIMENT 2: Outcomes of non-pharmacological management in ADHD-PI genetic targets and behavior

Rearing environment

From week 3 (PND 21) to 7 (PND 49-50), six mice were maintained in either the standard environment (SE) or EE (n=12). The onset and duration of the rearing environment were based on previous studies that reported improved neural and behavioral outcomes in spontaneously hypertensive rats (SHR/NCrl) [68, 69], the most validated animal model of ADHD. The overall cage size for both SE and EE measurements was 430 × 290 × 201 mm (L × B × H), with corncob bedding and a wire mesh cover. In addition, the EE cage contained a variety of stimulating, well-proportioned objects (i.e., colorful plastic tubes, wooden blocks, glass marbles, and small cylindrical-shaped wire cage platforms) (Figure 7b) to initiate interest and allow exploratory behavior, affording improvements in memory and cognitive functions [70, 71]. Cages were cleaned twice weekly to ensure a hygienic environment, and at the same time, objects in the EE group were rearranged into a novel configuration to ensure reinterest and re-exploration.

Treadmill exercise

The use of treadmill exercise allows an aerobic form of workout in mice, initiated in combination with EE, previously shown to improve memory and cognitive functions in rodents [72, 73, 74, 75]. Mice exposed to EE were allowed to run on a treadmill platform six times weekly (20 min/day) for four weeks in a rearing environment (Figure 7a).

Before the actual treadmill exercise, mice from the EE group were allowed a one-week adaptation period to familiarize themselves with the treadmill (Daejong Lab, Seoul, Republic of Korea). In the present study, we prevented the use of shock to stimulate running, as it may induce stress in mice, eventually altering their behavior. Instead, tapping with a wire brush was used to induce mice to continuous walking/running [76]. We maintained treadmill exercise for 20 min every six days, while the speed was gradually increased weekly to ensure continuous training and to stimulate running at the following speeds: week 0/habituation (10 m/20 min), week 1 (15 m/20 min), week 2 (20 m/min), week 3 (25 m/min), and week 4 (30 m/min). Mice experiencing early signs of fatigue (i.e., remaining still) were

allowed to rest and were eventually reintroduced to the platform to continue the remaining treadmill exercise period.

Y-maze

Separate groups of mice (THRSP OE, KO, WT) (n=12) were maintained in a SE (6 per cage) or EE (6 per cage) and subjected to Y-maze tests at a frequency of four tests conducted on days 7, 14, 21, and 28 of rearing enrichment (Figure 7a). The experimental protocols used were the same as those employed in Experiment 1 unless otherwise indicated.

Brain extraction

For mice (n=12) exposed to either SE or EE (Figure 7), brains were extracted and randomly assigned to two sets. The first set of six HPC samples was divided into left and right sections for subsequent use in qRT-PCR (left) and western blotting (right), whereas the last sets of brain samples were used for immunofluorescence (Figure 8-9).

RNA extraction and qRT-PCR

The left HPC isolated from the first set of mice exposed to either SE or EE was used for further RNA extraction and subsequent qRT-PCR analysis, using the same protocols as those in Experiment 1, unless otherwise indicated. In this experiment, we only measured and analyzed genes that were found to be altered during Experiment 1 or those showing up/downward trends. However, some genes were measured considering representation for each target belonging to ligands, inhibitors, receptors, co-receptors, and multiprotein complexes involved in canonical/non-canonical Wnt signaling. The gene targets, including Wnt3, Wnt6, Wnt7a, Cer1, Igfbp5, Wif1, Apcdd1, Fzd1, Fzd3, Lrp5, Lrp6, Ror1, Dvl1, Axin2, Csnk1 , Gsk3β, and Ctnnβ1 were normalized to Actb as the housekeeping gene.

Western blotting

Western blotting was performed on the right HPC isolated from the first set of mice exposed to the SE or EE to examine specific Wnt signaling targets (i.e., p-GSK3B, GSK3B, CSNK1E) (Figure 8i) and neuronal markers (i.e., NEU-N, GFAP) (Figure 9b) in the mouse hippocampal region using the same protocols as those used in Experiment 1.

5-BrdU injection

Mice were injected with 50 mg/kg 5-BrdU for 6 days during the last week of environmental enrichment and treadmill exercises (days 22–27), followed by a 100 mg/kg injection on day 28 after the behavioral experiments, or 3 h prior to brain extraction. This labeling technique targets proliferating cells in response to combined EE and treadmill exercise.

Immunofluorescence

Mice were sacrificed immediately after the last behavioral experiment and 5-BrdU injection. The protocols were the same as those used in Experiment 1, primarily targeting BrdU immunoreactivity (Figure 9a) in the hippocampal DG region.

Statistics and reproducibility

Statistical analyses were performed using GraphPad Prism v9.4 (GraphPad Software, Inc., La Jolla, CA, USA). For graphical purposes, data are presented as mean ± standard error of the mean, and all statistical analyses were conducted on raw data tested for normal (Gaussian) distribution using the D'Agostino-Pearson omnibus. The animal numbers and recorded data points are indicated in all figures. The results were analyzed using either one-way or two-way analysis of variance with or without repeated measures, followed by Tukey's multiple comparison test. A level of probability of $p \leq 0.05$ was defined as the threshold for statistical significance. Experiments were replicated at least three times.

Results

Hippocampal proteomic analysis in an ADHD-PI mouse model.

The inheritance of ADHD is deemed a complex phenomenon involving polygenic factors, accompanied by the development of distinct behavioral characteristics. Studies have shown that targeting a specific gene through genetic manipulation, as observed in transgenic models, intrinsically alters alternate genes by either upregulating or downregulating their expression levels, potentially inducing symptoms such as inattention, hyperactivity, and impulsivity. Previously, we have reported that THRSP overexpression in mice can produce attention and memory impairment related to dopaminergic [53] and thyroid hormones [52] aberrations, although other signaling mechanisms may also play a potential role. We conducted a proteomics analysis to provide a comprehensive representation of structural and functional data of the HPC, which plays a predominant role in cognitive functions, as well as the response mechanisms concerning genetic manipulations of THRSP in THRSP OE and KO mice.

The results revealed a total of 1780 differentially expressed proteins (DEPs) (Fig. 1c, Supplementary Table 1, 2) between THRSP KO and WT mice, with 681 and 1099 proteins upregulated and downregulated by 0.8-fold, respectively. Moreover, 1432 DEPs were observed between THRSP OE and WT (Fig. 1c, Supplementary Table 3, 4), where 600 proteins were upregulated by at least 0.8-fold and 832 were downregulated by 0.5-fold. Using this information, we applied the GENEONTOLOGY/PANTHER classification system to identify the GO biological processes involved in upregulated and downregulated proteins, and the total DEPs were analyzed to determine enriched pathways. GO analyses of DEPs in THRSP KO and OE mice identified variations in cellular processes, including localization, adhesion, and response to stimuli, as well as in metabolic and developmental processes (Fig. 2a-b; 3a-b). These biological processes may indicate the participation of NSC activity, which could be associated with hippocampal-dependent behaviors of these mice in the Y-maze test (Fig. 1a). Our previous and present data demonstrate that THRSP KO mice exhibit a high percentage of spontaneous alternations [52],

whereas THRSP OE mice (the ADHD-PI model) exhibited a low percentage of spontaneous alternations [52, 53], indicating a significant difference in their behavior probably attributed to functional deletion and overexpression of THRSP, respectively. However, whether NSCs are activated in response to their transgenic nature needs to be examined. Therefore, we conducted GO enrichment analysis and identified an enriched Wnt signaling pathway (Fig. 2c, 3c), where 36 genes from THRSP KO mice (Table 1) and 31 genes from THRSP OE mice (Table 2) demonstrated direct involvement in this signaling pathway. The data demonstrated the involvement of NSC activity in these THRSP transgenic mice, revealing that alterations in THRSP gene expression induce an inherent change in the expression of hippocampal Wnt-related proteins. Furthermore, we identified the enrichment of a pathway related to Rho-GTPase cytoskeletal regulation (Fig. 2c; 3c), previously identified as a key mediator of Wnt signaling [77]. Interestingly, THRSP OE mice presented variations in genes enriched in dopamine receptor signaling, supporting our previous findings that dopaminergic signaling is a factor underlying inattentive behavior [53].

The total DEPs used to produce GO biological processes were analyzed using STRING, presenting protein-protein interaction networks restricted to high-confidence (0.9) interaction thresholds (Fig. 2c; 3c) only. The protein network of DEPs from THRSP KO mice revealed the high interaction of catenin alpha 2 (CTNNA2) (Fig. 2c; highlighted in red). In contrast, DEPs in THRSP OE mice showed catenin beta 1 (CTNNB1) (Fig. 3c; highlighted in blue) to be among the most highly interacting proteins in the network. These critical findings provide evidence of differences between the two transgenic mice. However, THRSP OE mice are of particular interest, given the differential expression of CTNNB1 (upregulated), the key regulatory protein primarily involved in the formation of canonical Wnt/β-catenin signaling [78], in this inattentive and memory-impaired transgenic ADHD-PI model. It should be noted that Wnt/β-catenin signaling is speculated to control the balance of NSC proliferation and differentiation during brain development and adult neurogenesis [45, 46]. Disruption of Wnt signaling may result in developmental defects and neurological disorders [47], such as ADHD [10, 34, 48]. These observations showed an association between the upregulated expression of CTNNB1 and the ADHD-PI endophenotype in THRSP OE mice. Other important regulatory proteins were also found to be directly involved in canonical Wnt/β-catenin signaling, including adenomatous polyposis coli (APC) and casein kinase 1 alpha 1 (CSNK1A1), which are innately dysregulated in THRSP OE mice (Table 3). The current focus is on understanding how the upregulation of CTNNB1 affects the regulation of Wnt signaling and its targets and evaluating its contributory effects on hippocampal-dependent behavioral impairment in attention and memory in THRSP OE mice.

Aberrant Wnt-related genes in THRSP OE mice

We evaluated Wnt signaling-related markers upstream of CTNNB1, including the gene expression of hippocampal Wnt ligands, inhibitors, receptors, and co-receptors. Although CTNNB1 belongs to the canonical Wnt signaling, we also analyzed genes involved in the non-canonical pathway for an in-depth understanding of genetic changes in our THRSP OE mice, during which we also compared expressions of

gene targets with that of THRSP KO and WT mice. Among Wnt ligands measured, a significant reduction in Wnt7a gene expression was observed in THRSP OE mice when compared with both THRSP KO and WT mice (Fig. 4a-b). Other genes, including the canonical Wnt3 and Wnt8b ligands and non-canonical Wnt4, Wnt6, and Wnt11 ligands, demonstrated insignificant expression changes, although upward/downward trends were observed. Interestingly, the expression of Wnt inhibitors Cer1, Shisa9, and Apcdd1 was significantly higher in THRSP KO mice than in WT or THRSP OE mice. However, Wnt inhibitors such as Dkk4 and Igfbp5 were upregulated in THRSP OE mice.

Moreover, Wnt receptors Fzd1 and Fzd3 were increased in THRSP KO mice, whereas an upward trend was observed in THRSP OE mice when compared with WT mice. Wnt co-receptors of canonical signaling were deregulated and showed increased Lrp5 and Lrp10 expression in THRSP KO mice, whereas enhanced Lrp6 expression was observed in THRSP OE mice. Overall, these findings suggested that Wnt ligands, inhibitors, receptors, and co-receptors were deregulated in THRSP KO and THRSP OE mice without significantly enhancing Wnt ligands. In addition, upregulated DKk4 and Igfbp5 Wnt inhibitors present in THRSP OE mice could have affected the imbalance in Wnt receptors and co-receptors. This may also apply to observations from THRSP KO mice, demonstrating that the activation of Wnt ligands triggers altered expression of Wnt inhibitors, receptors, and co-receptors.

THRSP overexpression enhances some genes involved in (Wnt) multiprotein complex

The multiprotein complex in Wnt signaling regulates glycogen synthase kinase 3 (GSK3) activity by physically displacing complexed GSK3 from its original regulatory binding partners, APC and casein kinase 1 (CSNK1), and more recently, axin (AXIN), in the so-called destruction complex, consequently triggering the phosphorylation or degradation of β-catenin [79]. β-catenin is phosphorylated by the serine/threonine kinases CSNK1 and GSK3B and targeted for ubiquitination by the β-transducin repeat-containing protein (βTrCP) proteasomal degradation [80]. Following confirmation, in the absence of significant upregulation of Wnt ligands examined in THRSP OE mice, we subsequently assessed the multiprotein complex or the so-called destruction complex that further initiates either augmentation or degradation of β-catenin, deemed necessary for Wnt/β-catenin signaling. Herein, we observed that Axin2, Csnk1 , and Gsk3β were all enhanced in addition to the increased Ctnnβ1 and decreased Dvl1 gene expression levels (Fig. 5a). Moreover, the expression of hippocampal GSK3B and CSNK1E proteins was enhanced, confirming their enhanced gene expression. Additionally, GSK3B is considered to be constitutively inactivated by phosphorylation at Ser9 and activated by autophosphorylation at Tyr216 [81]. This finding indicates that the low phosphorylated GSK3B (Ser9) expression in THRSP OE mice confirms its high activity in the basal form, thereby impacting β-catenin expression.

THRSP OE mice exhibit impaired neurogenic markers

Wnt signaling regulates crucial aspects of NSC activity. Accordingly, we determined whether dysregulation of Wnt signaling in THRSP OE mice can impact the expression of select neurogenic markers in the HPC, particularly in the DG, which participates in the NSC neurogenic process in the adult

brain [65]. Immunofluorescence of HPC in THRSP OE mice presented a reduced percentage of DG cells expressing BrdU, along with decreased NEU-N and GFAP reactivity (Fig. 6a-b) when compared with that in THRSP KO and WT mice. Western blot analysis confirmed the reduced expression of NEU-N and GFAP (Fig. 6c) in THRSP OE mice, suggesting a possible maturational delay in NSCs and radial glial progenitor cells that could affect neuronal and glial formation in the nervous system during adult neurogenesis. In addition, these maturational delays in NSCs could have impacted the hippocampal-dependent behavioral performance of THRSP OE mice, resulting in inattention and memory impairment. Overall, the overexpression of THRSP in mice profoundly impacted the immunoreactivity and expression of neurogenic markers in the DG, implicated by impairments of Wnt/β-catenin signaling in THRSP OE mice.

EE and treadmill exercise ameliorate behavioral deficits in THRSP OE mice accompanied by improvements in Wnt signaling and NSC activity

Physiological effects of physical exercise on learning and memory have been demonstrated in human and animal models [82, 83], where regular physical exercise improves cognitive behavior by affording neuroprotective effects [84, 85]. Conversely, exposure to physically, mentally, and sensory stimulating (enriched) environments can improve learning and memory impairment [86]. All mice were exposed to EE combined with physical exercise for four weeks to evaluate these effects (Fig. 7a-b). Each group was exposed to a SE. Subsequently, these mice were exposed to the Y-maze, and the percentage of spontaneous alternations was analyzed, revealing an enhancement in attention and memory in mice, as evidenced by increased spontaneous alternations (Fig. 7c). Early exposure to an EE and physical activity improved cognitive behavior in mice, particularly in THRSP OE mice. This confirmed that ADHD-PI behavior could be improved by combining early environmental enrichment and physical exercise, supporting the use of non-pharmacological interventions to alleviate the signs and symptoms of ADHD [87, 88].

We previously identified the positive effects of combined environmental enrichment and physical exercise on attention and memory in mice, particularly in THRSP OE mice; herein, we aimed to investigate their effects on Wnt signaling and NSC activity. Compared with SE-exposed mice, groups exposed to combined EE and treadmill exercises showed improvement in the genetic markers of Wnt signaling. The expression levels of canonical Wnt3 and Wnt7a ligands were improved (Fig. 8a) in all strains, with accompanying reduction in canonical and non-canonical Cer1 and Igfbp5 Wnt inhibitors (Fig. 8c-d) in THRSP KO and OE, respectively. Interestingly, we noted an increase in Wnt receptors (Fzd3) (Fig. 8e) and co-receptors (Lrp5, Lrp6) (Fig. 8f) and signs of stabilization in the multiprotein complex targets by reducing the Csnk1 , Gsk3β, and Ctnnβ1 gene and protein expression levels (Fig. 8h-i). These results indicated that Wnt signaling activity was enhanced in the hippocampal region of mice exposed to combined EE and physical exercise, which may be related to improved attention and memory in mice during the Y-maze test. Furthermore, we detected the normalization of BrdU immunoreactivity (Fig. 9a) in THRSP OE mice, showing comparable percentages of DG cells expressing BrdU. Interestingly, NEU-N and GFAP expression improved (Fig. 9b), particularly in THRSP OE mice. Collectively, these findings suggested a relationship

between the inherent impairment of Wnt signaling, reduced NSC activity, inattention, and memory impairment in THRSP OE mice, which were improved by a combination of EE and treadmill exercises.

Discussion

Our study provides significant findings that could be valuable in advancing ADHD research. We identified hippocampal molecular signatures in an ADHD-PI mouse model that overexpressed THRSP rather than typical “culprits”, such as the dopaminergic hypothesis in ADHD or thyroid hormone dysfunction, also identified in our previous studies. Our current results converge with the ancient and evolutionary Wnt signaling pathways crucial for cell fate determination, migration, polarity, and neural patterning during neurodevelopment. These findings support the role of Wnt signaling in neurological disorders, particularly ADHD. Moreover, the integration of environmental enrichment with treadmill exercise has proven effective in improving not only behavior but also some altered molecular aspects in the hippocampal DG of THRSP OE mice, supporting the benefits conferred by non-pharmacological interventions, such as environmental modifications and exercise, in improving the signs and symptoms of ADHD.

It is interesting to note how functional overexpression and deletion of a certain gene, in this case, THRSP, would induce global differences not only in the behavior of mice but also in their molecular make-up. However, given that little is known regarding the function of THRSP in behavior, it remains unclear how genetic modifications in THRSP expression, particularly overexpression, but not KO, can induce ADHD-PI behavior. Two factors have been identified in our previous studies, i.e., dopaminergic [53] and thyroid hormone [52] aberrations, which are known to trigger ADHD development. The present findings indicating the involvement of impaired Wnt signaling afford a better understanding of the role of THRSP and how it induces ADHD-PI. One distinct functional role of THRSP is lipogenesis, where it acts as a lipogenic activator that eventually regulates the expression of several lipogenic genes [89]. This finding is of particular interest, given the role of lipogenesis in NSC activity.

In a key study, *de novo* lipogenesis, particularly fatty acid synthase (FASN) activity, was shown to be specifically elevated in mouse NSCs when compared with differentiated neuronal cells [90]. Lipogenesis is required for stem cell proliferation and, therefore, for normal neurogenesis to proceed. In contrast, THRSP and Spot14 have been identified as repressors of NSC proliferation [90]. THRSP decreases FASN activity by dimerizing with Mid1-Interacting G12-Like protein (MIG12), a THRSP homolog and activator of acetyl-CoA carboxylase (ACC), thereby inhibiting its function and decreasing ACC-mediated malonyl-CoA production, leading to a reduction in fatty acid synthesis [90]. Notably, cholesterol biosynthesis, known to occur through an independent pathway, is also required for NSC self-renewal and maintenance in the developing mouse forebrain, given that NSCs with mutations in enzymes involved in this pathway exhibit premature differentiation into neurons, thereby exhausting the stem cell pool [91].

Using *in situ* hybridization, THRSP-expressing cells were shown to constitute neural stem progenitor cells, [90, 92] confined to the adult brain [93] such as the subgranular zone of the hippocampal DG, which is highly neurogenic. Some progenitor cells are highly restricted to regions of the adult brain, such as the DG,

which plays a pivotal role in ensuring lifelong neurogenesis in the mammalian brain, necessary for improved learning, memory, and overall cognitive abilities [35, 94]. Indeed, changes in the production, growth, and overall regulation of new neurons in neurogenic brain regions have been associated with neuropsychiatric disorders, including ADHD [95, 96]. Remarkably, retroviral THRSP overexpression reduced hippocampal neural stem progenitor cell proliferation when compared with that induced by THRSP knockdown, indicating that THRSP plays a role in NSC modulation essential for neurogenesis. Therefore, THRSP overexpression and KO in mice potentially influence the expression of neuronal markers, indicative of the state of NSC activity in these transgenic mice, where THRSP OE mice exhibit reduced BrdU immunoreactivity with low NEU-N and GFAP protein expression when compared with THRSP KO mice with enhanced BrdU + cells and high NEU-N and GFAP expression. These effects might lead to altered or improved inattention or memory, which is evident in THRSP transgenic mice. In addition, THRSP is highly responsive to thyroid hormones, such as the neurogenic hippocampal DG.

Moreover, recent evidence has revealed that Wnt/β-catenin signaling participates in the regulation of thyroid hormone receptors, deiodinases, and transporter expression in target tissues, thereby affecting the transcriptional mechanisms [97]. Therefore, altered THRSP expression can induce aberrations, such as low thyroid hormone T3 levels. We have previously documented reduced T3 levels due to innately low monocarboxylate transporter 8 (MCT8) in these transgenic mice, [52] improved by thyroid hormone replacement (i.e., triiodothyronine/T3 [10 $mg \cdot kg^{-1}$], levothyroxine/T4 [10 $mg \cdot kg^{-1}$]), as evidenced by improvements in attention and memory behavior and theta wave normalization. Subsequently, this can alter the regulation of neuronal markers, as detected in the present study.

Our study is not the first to identify the role of impaired signaling in ADHD. However, to the best of our knowledge, this is the first study to use a specific animal model that could potentially improve our understanding of ADHD-PI. However, caution should be used when interpreting the observed findings, as only the hippocampal proteomes were evaluated, which may result in discrepant findings. Nonetheless, a few findings using *in vitro*, preclinical, and clinical samples have been previously reported, which can support and corroborate our findings. Among these, enhanced neuronal differentiation in cell models (i.e., murine neural stem, rat PC12, and human SH-SY5Y cells) has been associated with activation of Wnt signal transduction pathways, [34] induced by methylphenidate (Ritalin), a commonly used ADHD medication. We have previously reported that treatment with methylphenidate (5 $mg \cdot kg^{-1}$) could improve inattention during the Y-maze and novel-object recognition inTHRSP OE mice [53] This improved behavior in THRSP OE mice following methylphenidate injection could be attributed to Wnt signaling, as the classical G protein-coupled receptors and canonical Wnt pathways interact with each other by sharing several intermediate signaling components. Recent *in vivo* studies have revealed that antipsychotic drugs, known to dopamine D2-like receptors, increase cellular levels of downstream signaling components of canonical Wnt pathways, such as Dvl, Gsk3β, and Ctnnβ1, indicating functional interactions between the Wnt pathway and D2-like receptors [98]. Interestingly, these genetic markers were altered in THRPS-OE mice.

Additionally, the striatal transcriptomic analysis of an ADHD mouse model displaying hyperactivity and motor impulsivity revealed a pattern of synaptic remodeling. Subsequently, multiple genes were predicted to downregulate canonical Wnt pathways [10]. Lastly, an association study and meta-analysis have evaluated the involvement of canonical Wnt signaling LRP5 and LRP6 receptor gene variants in ADHD [48]. Interestingly, genetic variations in LRP5 intronic rs4988319 and rs3736228 (Ala1330Val) were observed among young females, whereas LRP6 rs2302685 (Val1062Ile) variations were observed in young males, indicating a potential sex-specific link between LRP5 and LRP6 gene variants in ADHD. In general, these recent findings support the hypothesis that genes involved in Wnt signaling might affect the physiology and predispose THRSP OE mice to ADHD-like symptoms.

Previous studies have shown that an active lifestyle involving regular exercise improves brain function, in which both synaptic plasticity and neurogenesis are modulated. In the mature brain, the canonical Wnt signaling pathway has been implicated in neuroprotection and synaptic plasticity. Herein, Wnt signaling was enhanced in THRSP OE mice, as evidenced by improvements in the expression of Wnt signaling-related markers that were previously altered. Moreover, long-term environmental enrichment accompanied by treadmill exercise improved the attention and memory of THRSP OE mice, concomitant with an improvement in Wnt signaling. Mice in the SE group showed lower expression levels of canonical Wnt ligands (i.e., Wnt3 and Wnt4) than the EE + treadmill groups, which exhibited higher expression levels. In addition, we noted improvements in the expression of Wnt receptors and co-receptors, particularly Fzd3 and Lrp5 mRNA levels, respectively, with low levels of Wnt inhibitors (i.e., Igfbp5, Apcdd1). Analysis of some components of the multiprotein complex implicated in the phosphorylation of β-catenin, resulting in either its proteasomal degradation or activation, exhibited low levels or reduced trends in Dvl1, Axin2, Csnk1ε, Gsk3β, and Ctnnβ1 mRNA in mice exposed to EE and treadmill exercise when compared with SE-exposed mice. Western blot analyses of p-GSK3B (Ser9) against basal GSK3B confirmed the high activity of the GSK3B basal form in THRSP OE SE-exposed mice; this was reversed by environmental enrichment and treadmill exercises, subsequently affecting the expression of β-catenin. Typically, Wnt ligands bind to cell surface-FZD/LRP5-6 receptor complexes, which then bind to Dvl, causing activation of the multiprotein complex or “destruction complex”; this, in turn, displaces GSK3B, preventing the phosphorylation and degradation of CTNNB1. Thus, our results suggest that activation of the Wnt signaling pathway induced by environmental enrichment and treadmill exercises enhances the behavior of THRSP OE mice, which is corroborated by a previous study [99].

Declarations

Authors’ contributions

RJPC was responsible for the study design. HJK and JHC supervised and funded the study. ECY and B-NK were also involved in the supervision of the studies. JK and ECY conducted the proteomic analysis. RJPC, DMO, LVS, HJL, DB, and MK performed data acquisition, analysis, and interpretation. RJPC drafted the manuscript. All the authors contributed to and approved the final version of the manuscript.

Data availability

Datasets generated and/or analyzed during the current study are available from the corresponding author upon reasonable request.

Acknowledgments

This work was supported by grants from the Bio & Medical Technology Development Program of the National Research Foundation (NRF) (2016R1D1A1B02010387; 2020M3E5D9080791) and Korea Health Technology R&D Project through the Korea Health Industry Development Institute (KHIDI), funded by the Ministry of Health & Welfare (HI19C0844) of the government of South Korea.

Competing interests

The authors declare no competing interests.

References

1. Felt BT, Biermann B, Christner JG, Kochhar P, Van Harrison R. Diagnosis and management of ADHD in children. American Family Physician **90**, 456–464 (2014).
2. Davidson MA. ADHD in adults: a review of the literature. Journal of Attention Disorders, (2008).
3. Luo Y, Weibman D, Halperin JM, Li X. A review of heterogeneity in attention deficit/hyperactivity disorder (ADHD). Frontiers in human neuroscience **13**, 42 (2019).
4. Song P, Zha M, Yang Q, Zhang Y, Li X, Rudan I. The prevalence of adult attention-deficit hyperactivity disorder: A global systematic review and meta-analysis. Journal of global health **11**, (2021).
5. Faraone SV, Larsson H. Genetics of attention deficit hyperactivity disorder. Molecular psychiatry **24**, 562–575 (2019).
6. Faraone SV, *et al.* Molecular genetics of attention-deficit/hyperactivity disorder. Biological psychiatry **57**, 1313–1323 (2005).
7. Grimm O, Kranz TM, Reif A. Genetics of ADHD: what should the clinician know? Current Psychiatry Reports **22**, 1–8 (2020).
8. Palladino VS, McNeill R, Reif A, Kittel-Schneider S. Genetic risk factors and gene–environment interactions in adult and childhood attention-deficit/hyperactivity disorder. Psychiatric genetics **29**, 63–78 (2019).
9. Østergaard SD, *et al.* Polygenic risk score, psychosocial environment and the risk of attention-deficit/hyperactivity disorder. Translational psychiatry **10**, 1–11 (2020).
10. Sorokina AM, *et al.* Striatal transcriptome of a mouse model of ADHD reveals a pattern of synaptic remodeling. PLoS One **13**, e0201553 (2018).
11. Gehricke J-G, *et al.* The brain anatomy of attention-deficit/hyperactivity disorder in young adults–a magnetic resonance imaging study. PloS one **12**, e0175433 (2017).

12. Mu S, Wu H, Zhang J, Chang C. Structural Brain Changes and Associated Symptoms of ADHD Subtypes in Children. Cerebral Cortex **32**, 1152–1158 (2022).
13. Ding L, Pang G. Identification of brain regions with enhanced functional connectivity with the cerebellum region in children with attention deficit hyperactivity disorder: a resting-state fMRI study. International journal of general medicine **14**, 2109 (2021).
14. Plessen KJ, *et al.* Hippocampus and amygdala morphology in attention-deficit/hyperactivity disorder. Archives of general psychiatry **63**, 795–807 (2006).
15. Rangarajan B, Suresh S, Mahanand B. Identification of potential biomarkers in the hippocampus region for the diagnosis of ADHD using PBL-McRBFN approach. In: 2014 *13th International Conference on Control Automation Robotics &* Vision *(ICARCV)*). IEEE (2014).
16. Al-Amin M, Zinchenko A, Geyer T. Hippocampal subfield volume changes in subtypes of attention deficit hyperactivity disorder. Brain research **1685**, 1–8 (2018).
17. Shaw P, Rabin C. New insights into attention-deficit/hyperactivity disorder using structural neuroimaging. Current psychiatry reports **11**, 393–398 (2009).
18. Posner J, Siciliano F, Wang Z, Liu J, Sonuga-Barke E, Greenhill L. A multimodal MRI study of the hippocampus in medication-naive children with ADHD: what connects ADHD and depression? Psychiatry Research: Neuroimaging **224**, 112–118 (2014).
19. Perlov E, *et al.* Hippocampus and amygdala morphology in adults with attention-deficit hyperactivity disorder. Journal of Psychiatry and Neuroscience **33**, 509–515 (2008).
20. Ike C, Pan MC, Thai CG, Alisso T. Attention-deficit/hyperactivity disorder predominantly inattentive subtype/presentation: Research progress and translational studies. Brain Sciences **10**, (2020).
21. Capdevila-Brophy C, Artigas-Pallarés J, Navarro-Pastor JB, García-Nonell K, Rigau-Ratera E, Obiols JE. ADHD predominantly inattentive subtype with high sluggish cognitive tempo: a new clinical entity? Journal of Attention Disorders **18**, 607–616 (2014).
22. Martinussen R, Tannock R. Working memory impairments in children with attention-deficit hyperactivity disorder with and without comorbid language learning disorders. Journal of clinical and experimental neuropsychology **28**, 1073–1094 (2006).
23. Chermak GD, Tucker E, Seikel JA. Behavioral characteristics of auditory processing disorder and attention-deficit hyperactivity disorder: predominantly inattentive type. Journal of the American Academy of Audiology **13**, 332–338 (2002).
24. Maurer AP, Nadel L. The continuity of context: A role for the hippocampus. Trends in Cognitive Sciences **25**, 187–199 (2021).
25. Kempermann G, *et al.* Human adult neurogenesis: evidence and remaining questions. Cell stem cell **23**, 25–30 (2018).
26. Bergmann O, Spalding KL, Frisén J. Adult neurogenesis in humans. Cold Spring Harbor perspectives in biology **7**, a018994 (2015).

27. Ihunwo AO, Tembo LH, Dzamalala C. The dynamics of adult neurogenesis in human hippocampus. Neural Regeneration Research **11**, 1869 (2016).
28. Kremer T, *et al.* Analysis of adult neurogenesis: evidence for a prominent “non-neurogenic” DCX-protein pool in rodent brain. PloS one **8**, e59269 (2013).
29. Vessal M, Aycock A, Garton MT, Ciferri M, Darian-Smith C. Adult neurogenesis in primate and rodent spinal cord: comparing a cervical dorsal rhizotomy with a dorsal column transection. European Journal of Neuroscience **26**, 2777–2794 (2007).
30. Zhao C, Deng W, Gage FH. Mechanisms and functional implications of adult neurogenesis. Cell **132**, 645–660 (2008).
31. Kempermann G, Wiskott L, Gage FH. Functional significance of adult neurogenesis. Current opinion in neurobiology **14**, 186–191 (2004).
32. Snyder JS. Recalibrating the relevance of adult neurogenesis. Trends in neurosciences **42**, 164–178 (2019).
33. Toda T, Gage FH. Adult neurogenesis contributes to hippocampal plasticity. Cell and tissue research **373**, 693–709 (2018).
34. Grünblatt E, Bartl J, Walitza S. Methylphenidate enhances neuronal differentiation and reduces proliferation concomitant to activation of Wnt signal transduction pathways. Translational psychiatry **8**, 1–13 (2018).
35. Homem CC, Repic M, Knoblich JA. Proliferation control in neural stem and progenitor cells. Nature Reviews Neuroscience **16**, 647–659 (2015).
36. Galvan A. Adolescence, brain maturation and mental health. Nature Neuroscience **20**, 503–504 (2017).
37. Kaufmann T, Alnæs D, Doan NT, Brandt CL, Andreassen OA, Westlye LT. Delayed stabilization and individualization in connectome development are related to psychiatric disorders. Nature neuroscience **20**, 513–515 (2017).
38. Mooney MA, *et al.* Pathway analysis in attention deficit hyperactivity disorder: an ensemble approach. American Journal of Medical Genetics Part B: Neuropsychiatric Genetics **171**, 815–826 (2016).
39. Poelmans G, Pauls DL, Buitelaar JK, Franke B. Integrated genome-wide association study findings: identification of a neurodevelopmental network for attention deficit hyperactivity disorder. American Journal of Psychiatry **168**, 365–377 (2011).
40. Nakka P, Raphael BJ, Ramachandran S. Gene and network analysis of common variants reveals novel associations in multiple complex diseases. Genetics **204**, 783–798 (2016).
41. Mulligan KA, Cheyette BN. Wnt signaling in vertebrate neural development and function. Journal of Neuroimmune Pharmacology **7**, 774–787 (2012).
42. Rosso SB, Inestrosa NC. WNT signaling in neuronal maturation and synaptogenesis. Frontiers in cellular neuroscience **7**, 103 (2013).

43. Arredondo SB, Valenzuela-Bezanilla D, Mardones MD, Varela-Nallar L. Role of Wnt signaling in adult hippocampal neurogenesis in health and disease. Frontiers in Cell and Developmental Biology, 860 (2020).
44. Salinas PC, Zou Y. Wnt signaling in neural circuit assembly. Annual review of neuroscience **31**, 339–358 (2008).
45. Komiya Y, Habas R. Wnt signal transduction pathways. Organogenesis **4**, 68–75 (2008).
46. Gao J, Liao Y, Qiu M, Shen W. Wnt/β-catenin signaling in neural stem cell homeostasis and neurological diseases. The Neuroscientist **27**, 58–72 (2021).
47. Okerlund ND, Cheyette BN. Synaptic Wnt signaling—a contributor to major psychiatric disorders? Journal of neurodevelopmental disorders **3**, 162–174 (2011).
48. Grünblatt E, *et al.* The involvement of the canonical Wnt-signaling receptor LRP5 and LRP6 gene variants with ADHD and sexual dimorphism: association study and meta-analysis. American Journal of Medical Genetics Part B: Neuropsychiatric Genetics **180**, 365–376 (2019).
49. Li Q, Meng Y, Wang J, Xie Y, Li T, Sun W. A Systematic Screening of ADHD-Susceptible Variants From 25 Chinese Parents–Offspring Trios. Frontiers in genetics **13**, (2022).
50. Shi X, *et al.* Ghrelin modulates dopaminergic neuron formation and attention deficit hyperactivity disorder-like behaviors: From animals to human models. Brain, Behavior, and Immunity **94**, 327–337 (2021).
51. Bem J, *et al.* Wnt/β-catenin signaling in brain development and mental disorders: keeping TCF7L2 in mind. FEBS letters **593**, 1654–1674 (2019).
52. Custodio RJP, *et al.* Low striatal T3 is implicated in inattention and memory impairment in an ADHD mouse model overexpressing thyroid hormone-responsive protein. Communications Biology **4**, 1101 (2021).
53. Custodio RJP, *et al.* Overexpression of the thyroid hormone-responsive (THRSP) gene in the striatum leads to the development of inattentive-like phenotype in mice. Neuroscience **390**, 141–150 (2018).
54. Hubrecht RC, Carter E. The 3Rs and humane experimental technique: implementing change. Animals **9**, 754 (2019).
55. Du Sert NP, *et al.* Reporting animal research: Explanation and elaboration for the ARRIVE guidelines 2.0. PLoS Biology **18**, e3000411 (2020).
56. Finlay BL, Darlington RB. Linked regularities in the development and evolution of mammalian brains. Science **268**, 1578–1584 (1995).
57. The Gene Ontology resource: enriching a GOld mine. Nucleic acids research **49**, D325-D334 (2021).
58. Ashburner M, *et al.* Gene ontology: tool for the unification of biology. Nature genetics **25**, 25–29 (2000).
59. Mi H, Muruganujan A, Ebert D, Huang X, Thomas PD. PANTHER version 14: more genomes, a new PANTHER GO-slim and improvements in enrichment analysis tools. Nucleic acids research **47**, D419-D426 (2019).

60. Szklarczyk D, *et al.* The STRING database in 2021: customizable protein–protein networks, and functional characterization of user-uploaded gene/measurement sets. Nucleic acids research **49**, D605-D612 (2021).
61. Custodio RJP, *et al.* Evaluation of the abuse potential of novel amphetamine derivatives with modifications on the amine (NBNA) and phenyl (EDA, PMEA, 2-APN) sites. Biomolecules & therapeutics **25**, 578 (2017).
62. Custodio RJP, *et al.* 25B-NBOMe, a novel N-2-methoxybenzyl-phenethylamine (NBOMe) derivative, may induce rewarding and reinforcing effects via a dopaminergic mechanism: Evidence of abuse potential. Addiction biology, e12850 (2019).
63. Custodio RJP, *et al.* Regulation of clock and clock-controlled genes during morphine reward and reinforcement: Involvement of the period 2 circadian clock. Journal of Psychopharmacology, 02698811221089040 (2022).
64. Franklin KB, Paxinos G. *The mouse brain in stereotaxic coordinates*. Academic press New York: (2008).
65. Braun SM, Jessberger S. Adult neurogenesis: mechanisms and functional significance. Development **141**, 1983–1986 (2014).
66. Custodio RJP, *et al.* Two newly-emerging substituted phenethylamines MAL and BOD induce differential psychopharmacological effects in rodents. Journal of Psychopharmacology **34**, 1056–1067 (2020).
67. Custodio RJ, *et al.* 5-HT2CR Is as Important as 5-HT2AR in Inducing Hallucinogenic Effects in Serotonergic Compounds. *Available at SSRN 4121838*.
68. Botanas CJ, *et al.* Rearing in an enriched environment attenuated hyperactivity and inattention in the spontaneously hypertensive rats, an animal model of attention-deficit hyperactivity disorder. Physiology & behavior **155**, 30–37 (2016).
69. Pamplona FA, Pandolfo P, Savoldi R, Prediger RDS, Takahashi RN. Environmental enrichment improves cognitive deficits in spontaneously hypertensive rats (SHR): relevance for attention deficit/hyperactivity disorder (ADHD). Progress in Neuro-Psychopharmacology and Biological Psychiatry **33**, 1153–1160 (2009).
70. Simpson J, Kelly JP. The impact of environmental enrichment in laboratory rats—behavioural and neurochemical aspects. Behavioural brain research **222**, 246–264 (2011).
71. Korkhin A, Zubedat S, Aga-Mizrachi S, Avital A. Developmental effects of environmental enrichment on selective and auditory sustained attention. Psychoneuroendocrinology **111**, 104479 (2020).
72. Hong M, *et al.* Treadmill exercise improves motor function and short-term memory by enhancing synaptic plasticity and neurogenesis in photothrombotic stroke mice. International Neurourology Journal **24**, S28 (2020).
73. Brenes JC, Fornaguera J, Sequeira-Cordero A. Environmental enrichment and physical exercise attenuate the depressive-like effects induced by social isolation stress in rats. Frontiers in Pharmacology, 804 (2020).

74. Wu S-Y, *et al.* Running exercise protects the substantia nigra dopaminergic neurons against inflammation-induced degeneration via the activation of BDNF signaling pathway. Brain, behavior, and immunity **25**, 135–146 (2011).
75. Kumar A, Rani A, Tchigranova O, Lee W-H, Foster TC. Influence of late-life exposure to environmental enrichment or exercise on hippocampal function and CA1 senescent physiology. Neurobiology of aging **33**, 828. e821-828. e817 (2012).
76. Dougherty JP, Springer DA, Gershengorn MC. The treadmill fatigue test: a simple, high-throughput assay of fatigue-like behavior for the mouse. JoVE (Journal of Visualized Experiments), e54052 (2016).
77. Schlessinger K, Hall A, Tolwinski N. Wnt signaling pathways meet Rho GTPases. Genes & development **23**, 265–277 (2009).
78. Willert K, Nusse R. β-catenin: a key mediator of Wnt signaling. Current opinion in genetics & development **8**, 95–102 (1998).
79. Nusse R. Wnt signaling in disease and in development. Cell research **15**, 28–32 (2005).
80. Stamos JL, Weis WI. The β-catenin destruction complex. Cold Spring Harbor perspectives in biology **5**, a007898 (2013).
81. Krishnankutty A, *et al.* In vivo regulation of glycogen synthase kinase 3β activity in neurons and brains. Scientific Reports **7**, 1–15 (2017).
82. Kreft H, Jetz W. Global patterns and determinants of vascular plant diversity. *Proceedings of the National Academy of Sciences* **104**, 5925–5930 (2007).
83. van Dongen EV, Kersten IH, Wagner IC, Morris RG, Fernández G. Physical exercise performed four hours after learning improves memory retention and increases hippocampal pattern similarity during retrieval. Current Biology **26**, 1722–1727 (2016).
84. Joubert C, Chainay H. Aging brain: the effect of combined cognitive and physical training on cognition as compared to cognitive and physical training alone–a systematic review. Clinical interventions in aging **13**, 1267 (2018).
85. Lago TR, *et al.* Exercise modulates the interaction between cognition and anxiety in humans. Cognition and Emotion **33**, 863–870 (2019).
86. Mora-Gallegos A, Rojas-Carvajal M, Salas S, Saborío-Arce A, Fornaguera-Trías J, Brenes JC. Age-dependent effects of environmental enrichment on spatial memory and neurochemistry. Neurobiology of learning and memory **118**, 96–104 (2015).
87. Young S, Myanthi Amarasinghe J. Practitioner Review: Non-pharmacological treatments for ADHD: A lifespan approach. Journal of Child Psychology and Psychiatry **51**, 116–133 (2010).
88. Sonuga-Barke EJ, *et al.* Nonpharmacological interventions for ADHD: systematic review and meta-analyses of randomized controlled trials of dietary and psychological treatments. American Journal of Psychiatry **170**, 275–289 (2013).

89. Ren J, *et al.* Expression of thyroid hormone responsive SPOT 14 gene is regulated by estrogen in chicken (Gallus gallus). Scientific Reports **7**, 1–10 (2017).
90. Knobloch M, *et al.* Metabolic control of adult neural stem cell activity by Fasn-dependent lipogenesis. Nature **493**, 226–230 (2013).
91. Driver AM, Kratz LE, Kelley RI, Stottmann RW. Altered cholesterol biosynthesis causes precocious neurogenesis in the developing mouse forebrain. Neurobiology of disease **91**, 69–82 (2016).
92. Knobloch M, von Schoultz C, Zurkirchen L, Braun SM, Vidmar M, Jessberger S. SPOT14-positive neural stem/progenitor cells in the hippocampus respond dynamically to neurogenic regulators. Stem cell reports **3**, 735–742 (2014).
93. Lemkine G, *et al.* Adult neural stem cell cycling in vivo requires thyroid hormone and its alpha receptor. The FASEB journal **19**, 1–17 (2005).
94. Aimone JB, Li Y, Lee SW, Clemenson GD, Deng W, Gage FH. Regulation and function of adult neurogenesis: from genes to cognition. Physiological reviews **94**, 991–1026 (2014).
95. Wulaer B, *et al.* Shati/Nat8l deficiency disrupts adult neurogenesis and causes attentional impairment through dopaminergic neuronal dysfunction in the dentate gyrus. Journal of neurochemistry, (2020).
96. Fredriksson A, Archer T. Neurobehavioural deficits associated with apoptotic neurodegeneration and vulnerability for ADHD. Neurotoxicity research **6**, 435–456 (2004).
97. Skah S, Uchuya-Castillo J, Sirakov M, Plateroti M. The thyroid hormone nuclear receptors and the Wnt/β-catenin pathway: An intriguing liaison. Developmental biology **422**, 71–82 (2017).
98. Min C, Cho D-I, Kwon K-J, Kim K-S, Shin CY, Kim K-M. Novel regulatory mechanism of canonical Wnt signaling by dopamine D2 receptor through direct interaction with β-catenin. Molecular pharmacology **80**, 68–78 (2011).
99. Bayod S, *et al.* Wnt pathway regulation by long-term moderate exercise in rat hippocampus. Brain Research **1543**, 38–48 (2014).

Tables

Tables 1-3 are in the supplementary files section.

Figures

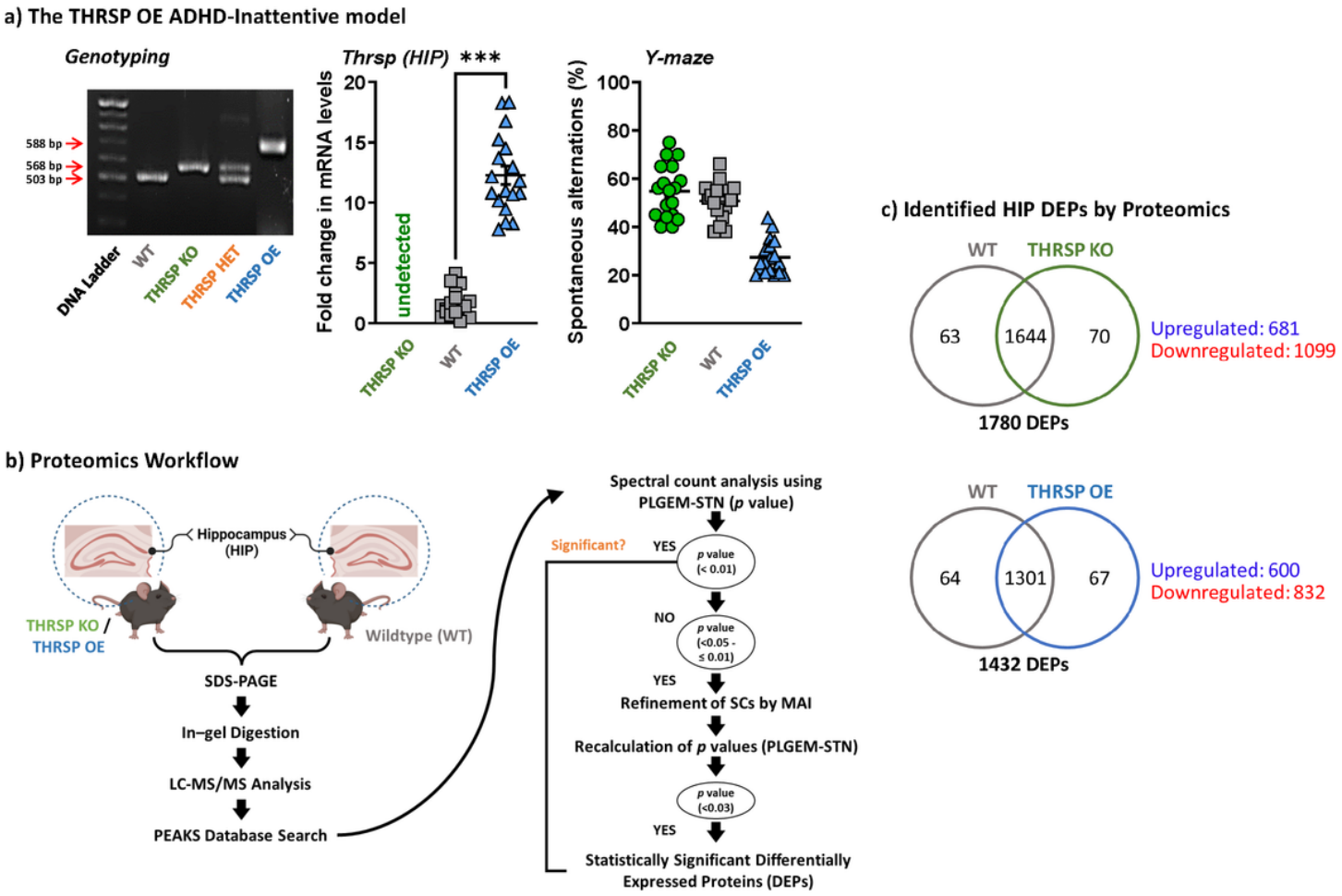

Figure 1

Proteomics workflow in THRSP transgenic mice. a) Confirmation of transgenic backgrounds in mice was performed via DNA electrophoresis (Genotyping) and qRT-PCR (Thrsp mRNA expression) analyses (n = 18 mice/group, two-tailed, paired t-test; (t=11.9, df=17, P < 0.001)). Thrsp mRNA was not detected in THRSP KO mice. Subsequently, mice were exposed to the Y-maze test to reconfirm inattention in THRSP OE mice when compared to WT and THRSP KO mice (n = 18 mice/group; one-way ANOVA, F (2, 51) = 51.7, P < 0.001). THRSP OE mice show sustained inattention and memory impairments. Values are presented as the mean ± standard error of the mean (SEM) b) Following the confirmation of behavior in mice, brain samples from the hippocampus (HPC) were prepared for subsequent proteomics analysis. C) Summary of identified differentially expressed proteins (DEP) in mouse HPC. KO, knockout; OE, overexpressing; THRSP, thyroid hormone-responsive protein; WT, wild-type.

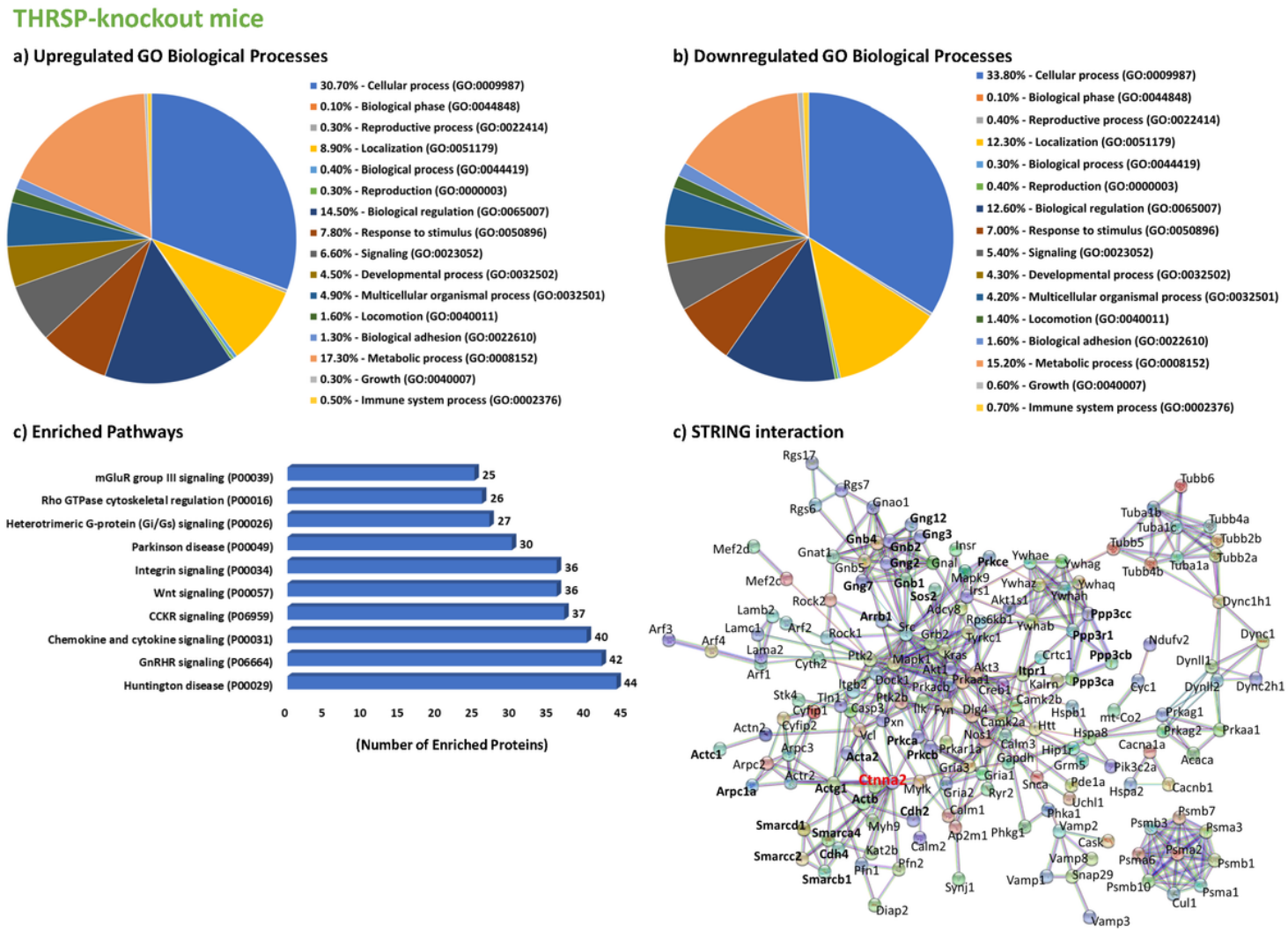

Figure 2

Proteomics analysis of the HPC in THRSP KO mice. a-b) The Gene Ontology biological processes of upregulated and downregulated proteins in the hippocampus (HPC) of adult THRSP KO mice. In total, 681 and 1099 proteins are upregulated and downregulated by 0.8-fold, respectively. c) Reactome pathway enrichment analysis using upregulated and downregulated proteins identified from the proteomics screen. d) STRING protein-protein interaction network analysis indicates that Ctnna2 (marked in red), the only gene directly related to Wnt signaling, is highly interacting. Although, other Wnt signaling-related proteins were identified to exhibit an interaction. KO, knockout; THRSP, thyroid hormone-responsive protein.

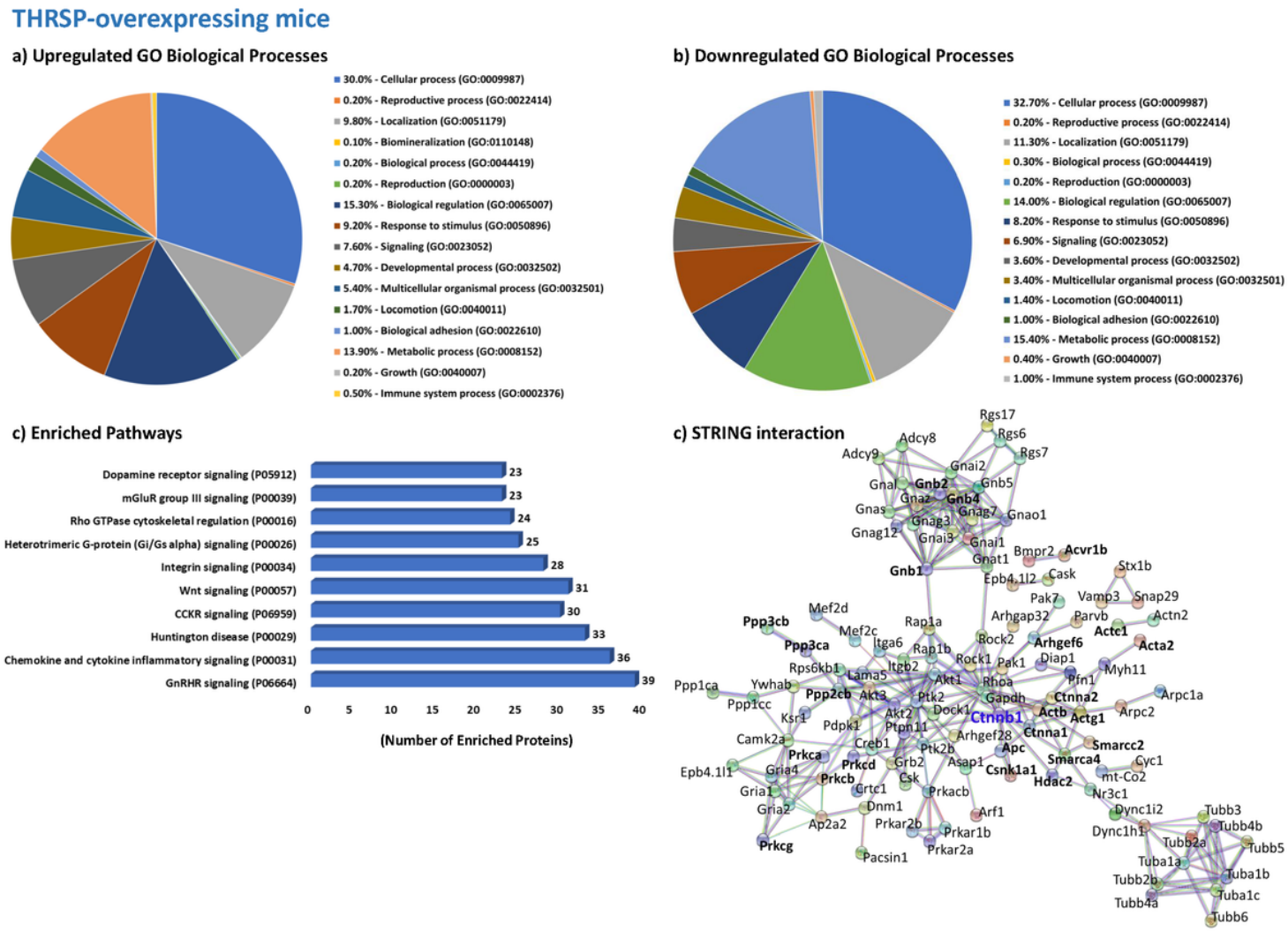

Figure 3

Proteomics analysis of the HPC in THRSP OE mice. a-b) The Gene Ontology biological processes of upregulated and downregulated proteins in the HPC of adult THRSP OE mice. In total, 600 proteins are upregulated by at least 0.8-fold, whereas 832 proteins are downregulated by 0.5-fold. c) Reactome pathway enrichment analysis using upregulated and downregulated proteins identified from the proteomics screen. d) STRING protein-protein interaction network analysis indicates enriched interactions indicate Ctnnb1 (marked in blue) as the most highly interacting protein, although other Wnt signaling-related proteins were identified. HPC, hippocampus; OE, overexpressing; THRSP, thyroid hormone-responsive protein.

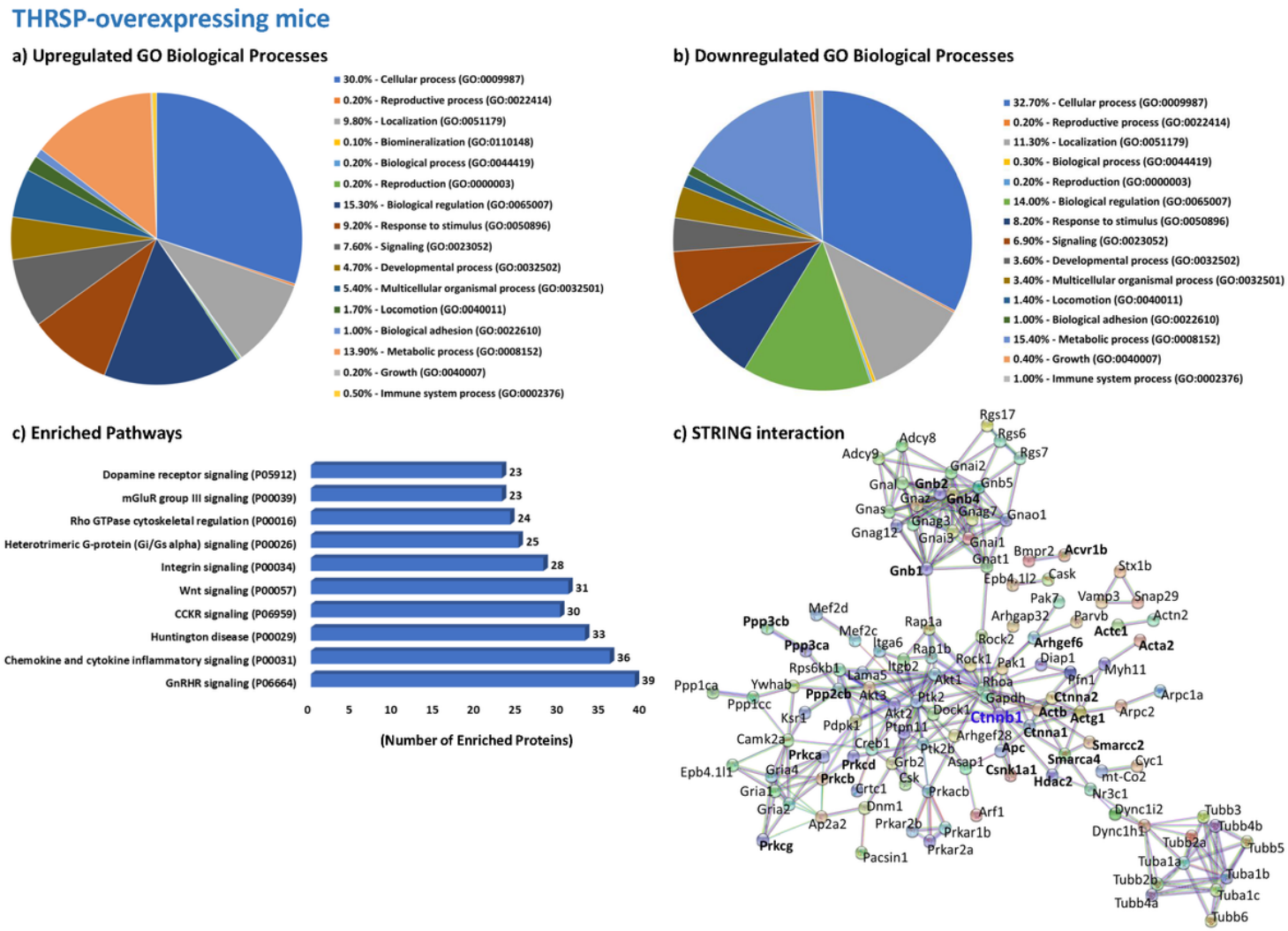

Figure 3

Proteomics analysis of the HPC in THRSP OE mice. a-b) The Gene Ontology biological processes of upregulated and downregulated proteins in the HPC of adult THRSP OE mice. In total, 600 proteins are upregulated by at least 0.8-fold, whereas 832 proteins are downregulated by 0.5-fold. c) Reactome pathway enrichment analysis using upregulated and downregulated proteins identified from the proteomics screen. d) STRING protein-protein interaction network analysis indicates enriched interactions indicate Ctnnb1 (marked in blue) as the most highly interacting protein, although other Wnt signaling-related proteins were identified. HPC, hippocampus; OE, overexpressing; THRSP, thyroid hormone-responsive protein.

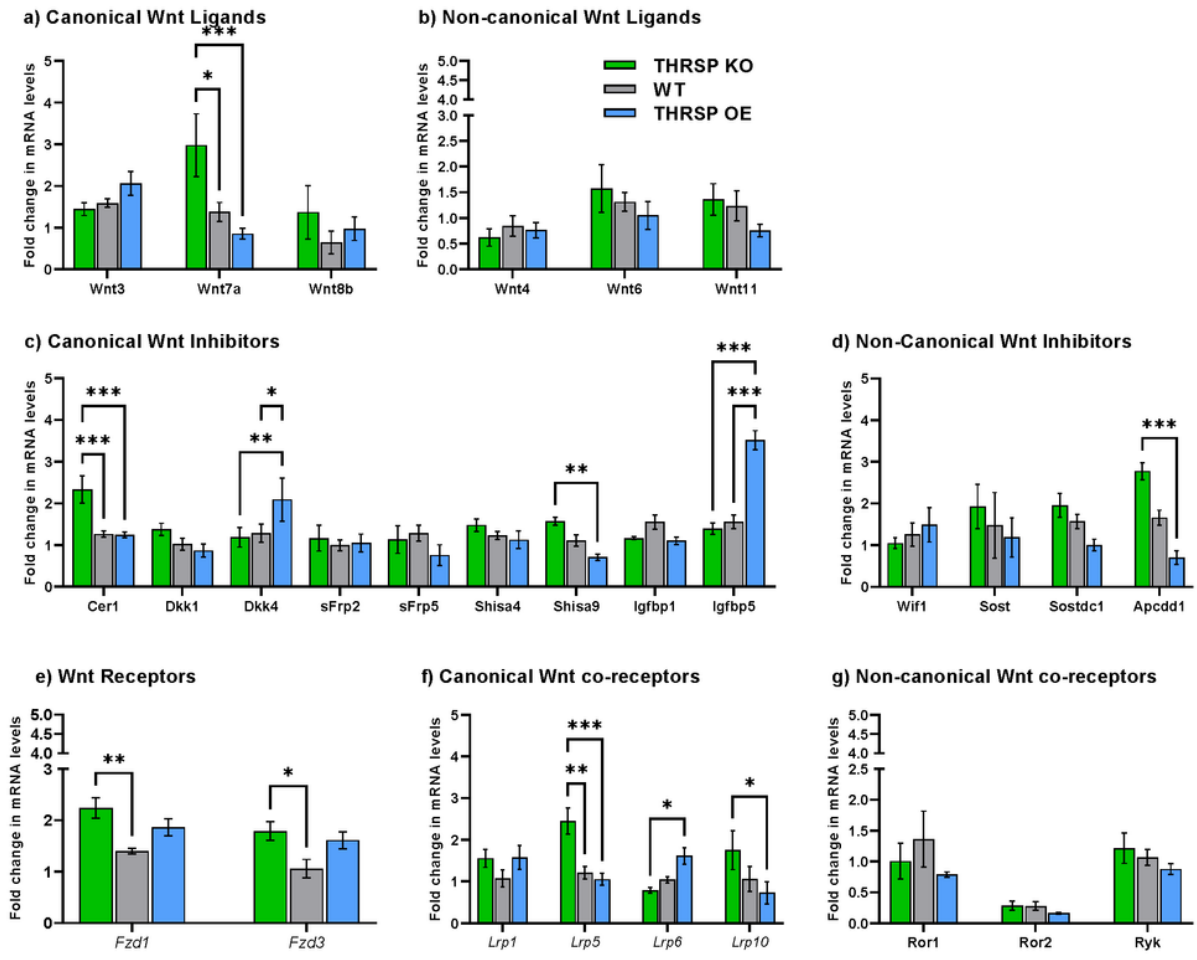

Figure 4

Canonical and non-canonical Wnt pathway elements expressions in the mouse hippocampus. qRT-PCR analyses of a) canonical and b) non-canonical Wnt ligands (n = 6 mice/group; a) two-way ANOVA, Strain: $F(2, 45) = 3.24$, $P = 0.048$; Gene targets: $F(2, 45) = 3.58$, $P = 0.036$; Strain × Gene targets: $F(4, 45) = 3.41$, $P = 0.016$; b) two-way ANOVA, Strain: $F(2, 44) = 1.35$, $P = 0.269$; Gene targets: $F(2, 44) = 3.53$, $P = 0.038$; Strain × Gene targets: $F(4, 44) = 0.626$, $P = 0.647$). The mRNA expression levels of c) canonical and d) non-canonical Wnt inhibitors (n = 6 mice/group; c) two-way ANOVA, Strain: $F(2, 133) = 1.70$, $P = 0.186$; Gene targets: $F(8, 133) = 9.61$, $P < 0.001$; Strain × Gene targets: $F(16, 133) = 7.31$, $P < 0.001$; d) two-way ANOVA, Strain: $F(2, 60) = 5.16$, $P = 0.009$; Gene targets: $F(3, 60) = 0.754$, $P = 0.524$; Strain × Gene targets: $F(6, 60) = 1.99$, $P = 0.081$). mRNA levels of e) Wnt receptors, f) canonical Wnt co-receptors, and g) non-canonical Wnt co-receptors. e) Two-way ANOVA, Strain: $F(2, 24) = 11.18$, $P < 0.001$; Gene targets: $F(1, 24) = 6.67$, $P = 0.0.16$; Strain × Gene targets: $F(2, 24) = 0.182$, $P = 0.835$; f) two-way ANOVA, Strain: $F(2, 59) = 5.33$, $P = 0.007$; Gene targets: $F(3, 59) = 2.10$, $P = 0.110$; Strain × Gene targets: $F(6, 59) = 4.76$, $P < 0.001$; g) two-way ANOVA, Strain: $F(2, 45) = 1.64$, $P = 0.205$; Gene targets: $F(2, 45) = 15.2$, $P < 0.001$; Strain × Gene targets: $F(4, 45) = 0.546$, $P = 0.703$). Values are presented as the mean ± standard error of

the mean (SEM). Data show differential expression of canonical and non-canonical Wnt pathway elements.

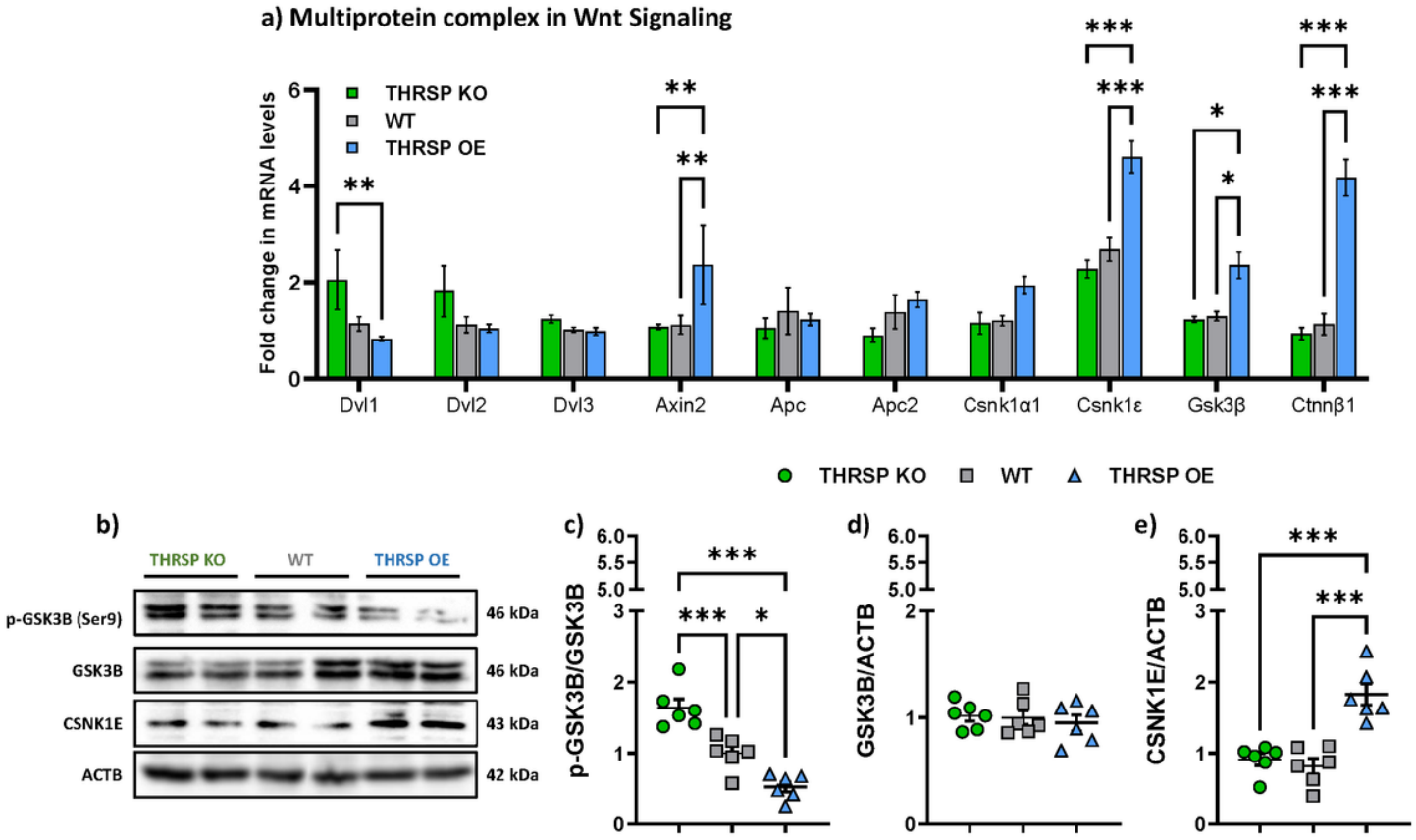

Figure 5

Differential expressions of Wnt signaling multiprotein complex in the mouse hippocampus. a) qRT-PCR analyses of multiprotein complexes, b) Representative western blots, and corresponding protein levels of c) p-GSK3B, d) GSK3B, and e) CSNK1E, the primary mediators of β-catenin phophorylation. (n = 6 mice/group; a) two-way ANOVA, Strain: $F(2, 150) = 22.7$, $P < 0.001$; Gene targets: $F(9, 150) = 13.7$, $P < 0.001$; Strain × Gene targets: $F(18, 150) = 6.47$, $P < 0.001$). c) one-way ANOVA, $F(2, 15) = 32.3$, $P < 0.001$; d) one-way ANOVA, $F(2, 15) = 0.294$, $P = 0.750$; e) one-way ANOVA, $F(2, 15) = 22.5$, $P < 0.001$). Values are presented as the mean ± standard error of the mean (SEM). Data indicate low expression of phosphorylated GSK3B (Ser9) in THRSP OE mice, confirming basal hyperactivity of GSK3B that could subsequently affect β-catenin. OE, overexpressing; THRSP, thyroid hormone-responsive protein.

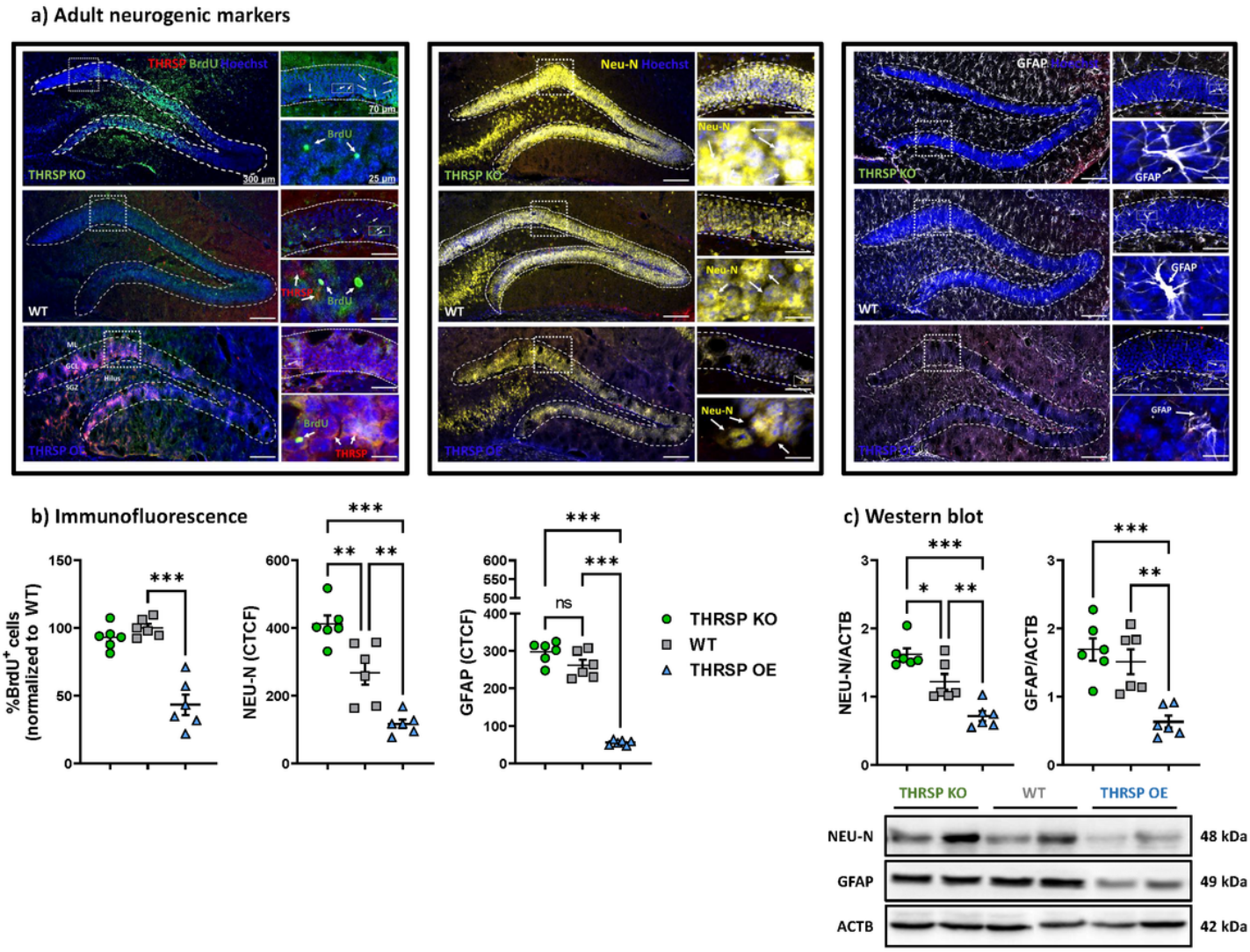

Figure 6

Differential expression of hippocampal DG nurogenic markers. a) Representative fluorescence immunoreactivity of BrdU, NEU-N, and GFAP in mouse hippocampal DG, and their b) corresponding analyses, and separate protein analyses using c) western blotting. (n = 6 mice/group; b) one-way ANOVA, %BrdU+ cells: $F(2, 15) = 38.9$, $P < 0.001$; NEU-N (CTCF): $F(2, 15) = 32.0$, $P < 0.001$; GFAP (CTCF): $F(2, 15) = 147$, $P < 0.001$). c) one-way ANOVA, NEU-N/ACTB: $F(2, 15) = 23.6$, $P < 0.001$; GFAP/ACTB, $F(2, 15) = 14.0$, $P < 0.001$). Values are presented as the mean ± standard error of the mean (SEM). Data show impaired neural stem cell proliferation in THRSP OE mice. DG, dentate gyrus; OE, overexpressing; THRSP, thyroid hormone-responsive protein.

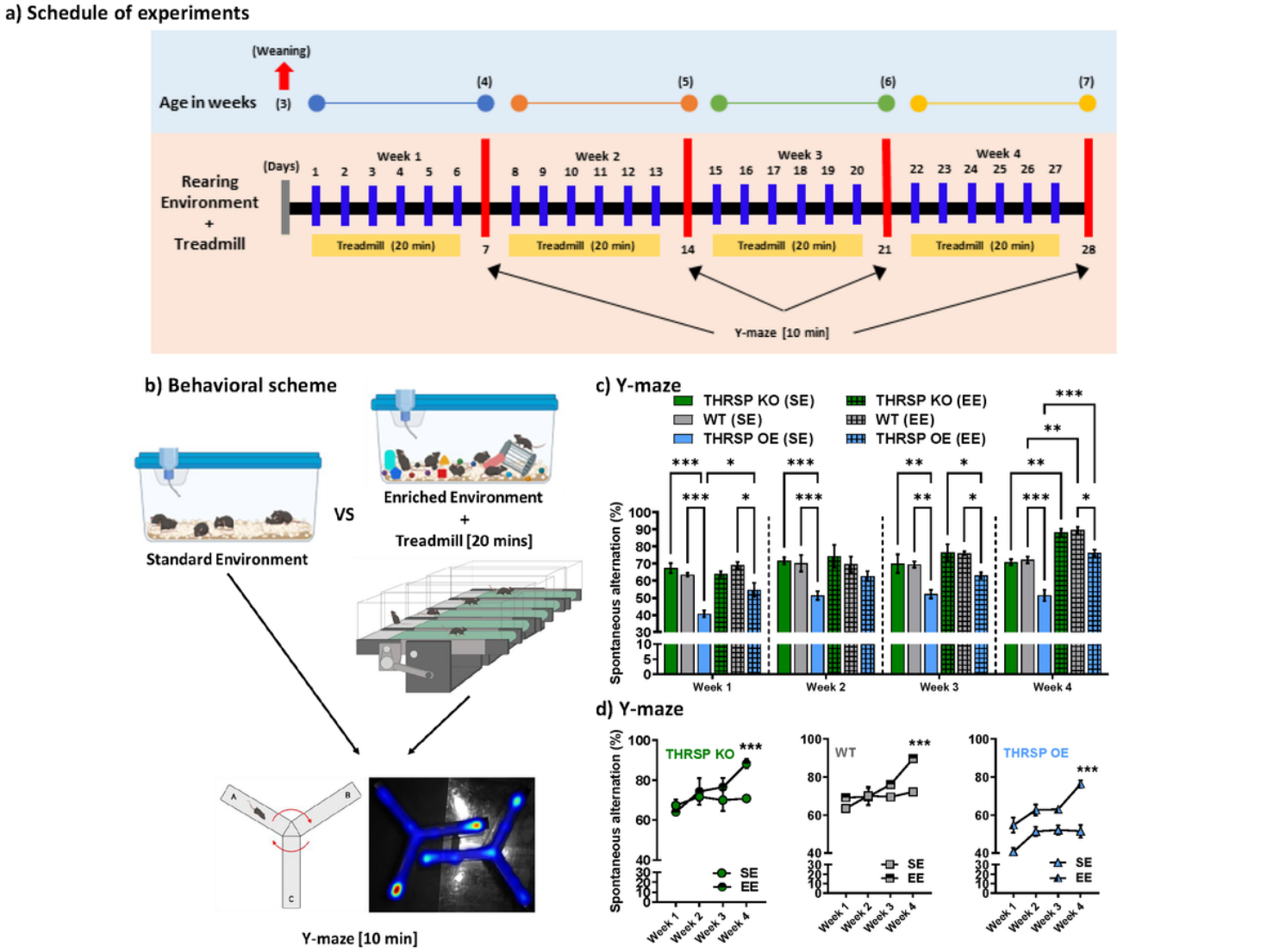

Figure 7

Effects of combined environmental enrichment and treadmill exercises on the ADHD-PI-like behavior in THRSP OE mice. a) Experimental schedule showing age in weeks and the commencement of of rearing environment + treadmill exercises in mice. b) Behavioral scheme showing the representative image, with cages where mice were exposed (standard *vs.* enriched environment), treadmill, and representative Y-maze heatmap image. c-d) The behavior of mice exposed to SE and EE throughout the 4-week exposure to rearing environment + treadmill exercises. (n = 12 mice/group; c) one-way ANOVA, $F(5, 18) = 7.62$, $P < 0.001$); d) two-way ANOVA (THRSP KO), Weeks: $F(1, 22) = 6.32$, $P = 0.020$; SE/EE exposure per strain: $F(1.72, 37.8) = 3.99$, $P = 0.032$; Weeks × SE/EE exposure per strain: $F(3, 66) = 2.37$, $P = 0.078$); e) two-way ANOVA (THRSP KO), Weeks: $F(1, 44) = 15.8$, $P < 0.001$; SE/EE exposure per strain: $F(3, 44) = 9.69$, $P < 0.001$; Weeks × SE/EE exposure per strain: $F(3, 44) = 4.16$, $P = 0.011$); f) two-way ANOVA (THRSP KO), Weeks: $F(1, 44) = 46.5$, $P < 0.001$; SE/EE exposure per strain: $F(3, 44) = 19.5$, $P < 0.001$; Weeks × SE/EE exposure per strain: $F(3, 44) = 2.14$, $P = 0.109$). Values are presented as the mean ± standard error of the mean (SEM). Environmental enrichment and treadmill exercise ameliorate behavioral deficits in THRSP OE mice. ADHD-PI, Attention deficit hyperactivity disorder predominantly inattentive; EE, enriched

environment; KO, knockout; OE, overexpressing; SE, standard environment; THRSP, thyroid hormone-responsive protein.

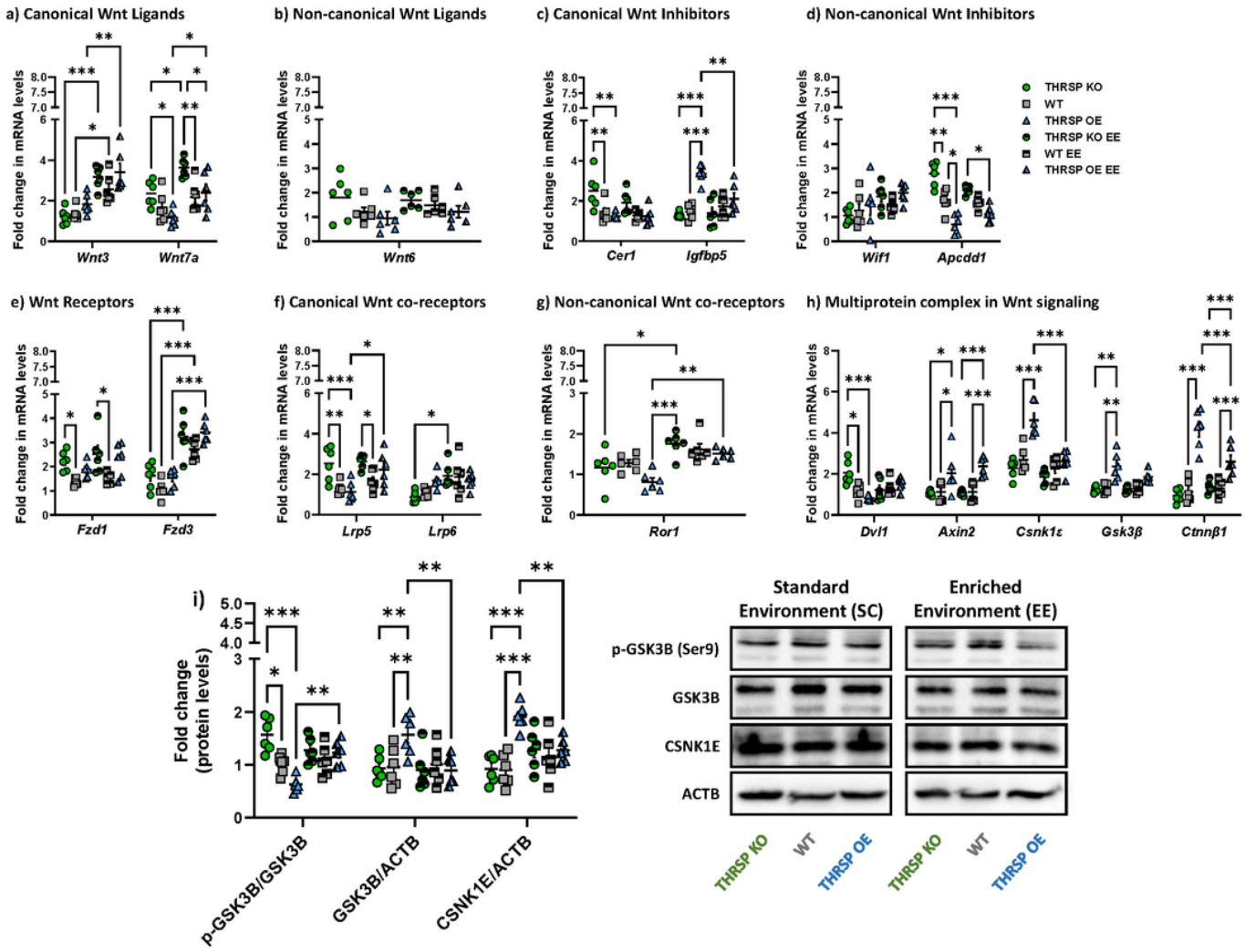

Figure 8

Expression of hippocampal Wnt pathway elements after environmental enrichment and treadmill exercises. qRT-PCR analyses of a) canonical and b) non-canonical Wnt ligands (n = 6 mice/group; a) two-way ANOVA, Strain: $F(5, 60) = 17.0$, $P < 0.001$, Gene targets: $F(1, 60) = 0.0245$, $P = 0.876$; Strain × Gene targets: $F(5, 60) = 4.51$, $P = 0.001$; b) one-way ANOVA, $F(5, 30) = 1.82$, $P = 0.139$), the c) canonical and d) non-canonical Wnt inhibitors (n = 6 mice/group; a) two-way ANOVA, Strain: $F(5, 60) = 4.35$, $P = 0.002$, Gene targets: $F(1, 60) = 5.72$, $P = 0.020$; Strain × Gene targets: $F(5, 60) = 4.51$, $P < 0.001$; b) two-way ANOVA, Strain: $F(5, 60) = 5.18$, $P < 0.001$, Gene targets: $F(1, 60) = 1.63$, $P = 0.207$; Strain × Gene targets: $F(5, 60) = 11.1$, $P < 0.001$), and the mRNA expression levels of e) Wnt receptors, f) canonical, g) non-canonical Wnt co-receptors, and h) the Wnt signaling multiprotein complex (n = 6 mice/group; e) two-way ANOVA, Strain: $F(5, 60) = 20.6$, $P < 0.001$, Gene targets: $F(1, 60) = 6.38$, $P = 0.014$; Strain × Gene targets: $F(5, 60) = 7.70$, $P < 0.001$; f) two-way ANOVA, Strain: $F(5, 60) = 5.52$, $P < 0.001$, Gene targets: $F(1, 60) =$

8.80, P = 0.004; Strain × Gene targets: F (5, 60) = 5.81, P < 0.001); g) one-way ANOVA, F (5, 30) = 8.30, P < 0.001; f) two-way ANOVA, Strain: F (5, 150) = 40.6, P < 0.001, Gene targets: F (4, 150) = 45.6, P < 0.001; Strain × Gene targets: F (20, 150) = 9.67, P < 0.001). Confirmation of protein levels of some i) mediators in the multiprotein complex (p-GSK3B, GSK3B, CSNK1E) (n = 6 mice/group; two-way ANOVA, SE/E exposure per strain: F (5, 90) = 3.58, P = 0.005, Gene targets: F (2, 90) = 4.01, P = 0.022; SE/E exposure per strain × Gene targets: F (10, 90) = 8.34, P < 0.001). Values are presented as the mean ± standard error of the mean (SEM). Environmental enrichment and treadmill exercise improve the Wnt signaling in mice. EE, enriched environment; SE, standard environment.

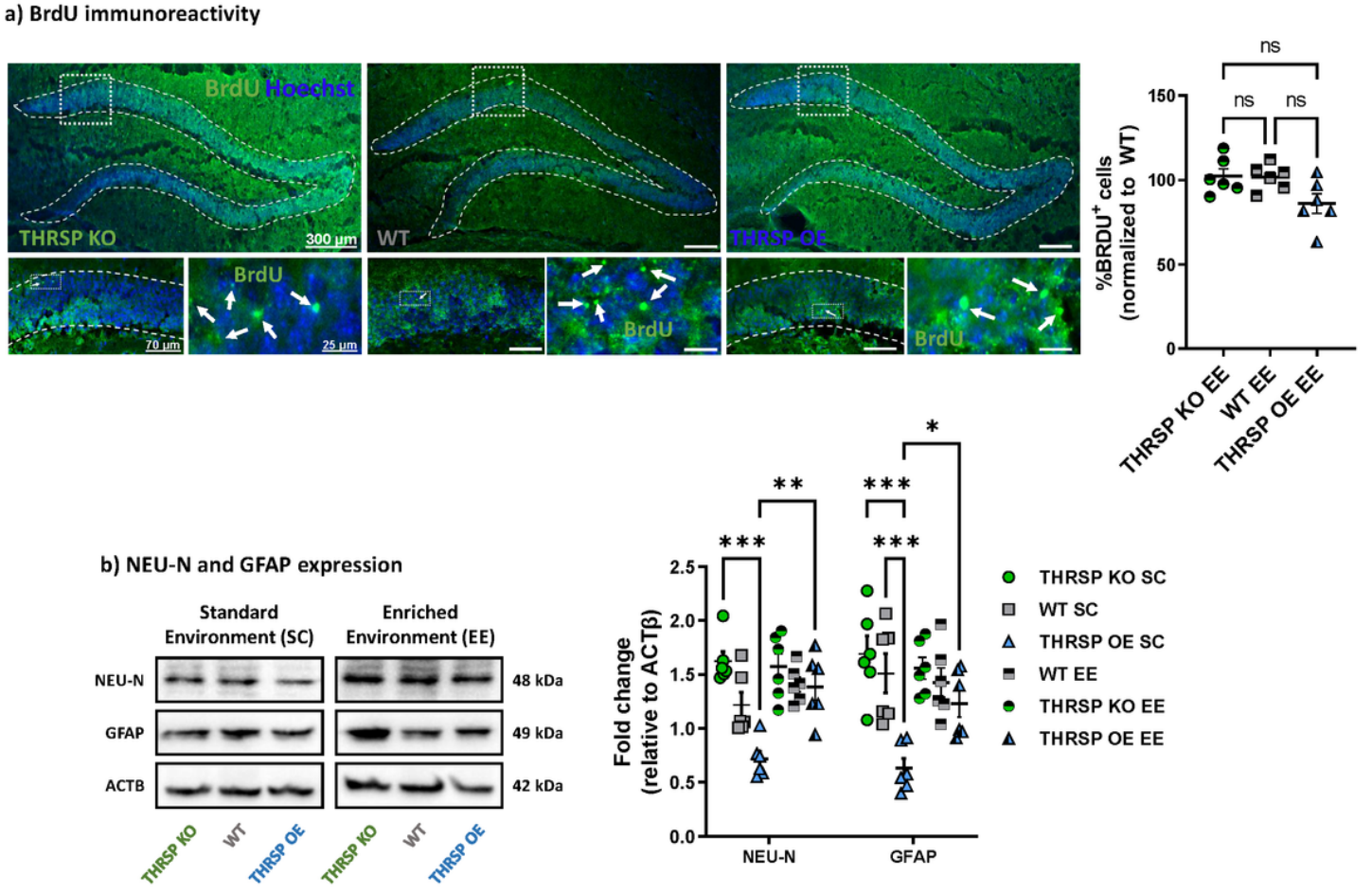

Figure 9

Regulation of hippocampal neurogenic markers after environmental enrichment and treadmill exercises. a) BrdU immunoreactivity and b) protein expression levels of NEU-N and GFAP in the mouse hippocampal DG. (n = 6 mice/group; a) one-way ANOVA, F (2, 15) = 4.02, P = 0.040; b) two-way ANOVA, SE/E exposure per strain: F (5, 60) = 16.6, P < 0.001, Protein targets: F (1, 60) = 0.0916, P = 0.763; SE/E exposure per strain × Protein targets: F (5, 60) = 0.820, P = 0.540). Values are presented as the mean ± S.E.M. Enriched

environment and treadmill exercises improves in NSC activity in THRSP via normalization of neurogenic markers. DG, dentate gyrus; EE, enriched environment; NSC, neural stem cell; SE, standard environment; THRSP, thyroid hormone-responsive protein.

Supplementary Files

This is a list of supplementary files associated with this preprint. Click to download.

- Table1.pdf
- Table2.pdf
- Table3.pdf
- Table2.pdf
- SupplementaryTables.xlsx